Electronic Supplementary Material (ESI) for ChemComm.

Supporting Information for

A Catalytically Relevant Intermediate in the Synthesis of Cyclic Polymers from Alkynes

Christopher D. Roland, Tianyu Zhang, Sudarsan VenkatRamani, Ion Ghiviriga, and Adam S. Veige*

University of Florida, Department of Chemistry, Center for Catalysis, P.O. Box 117200, Gainesville, FL, 32611.

Table of Contents

General Considerations

Unless specified otherwise, all manipulations were performed under an inert atmosphere using glove-box techniques. Toluene and pentane were dried using a GlassCountour drying column. Phenylacetylene was purchased from Sigma-Aldrich, distilled from magnesium sulfate, degassed by freeze pump thawing, and filtered through a column of basic alumina immediately prior to use. Toluene-d_8 was dried over phosphorous pentoxide (P_2O_5), distilled, degassed by freeze pump thawing, and stored over 4Å molecular sieves. $[O_2C(^tBuC{=})W(\eta^2\text{-}HC{\equiv}C^tBu)(THF)]$ (**1**)[1,2] and $[^tBuOCO]W{\equiv}C^tBu(THF)_2$ (**3**)[3] were prepared according to literature procedure. Linear polyphenyacetylene was prepared according to literature methods.[4,5] NMR spectra were obtained on Varian INOVA 500 MHz and Varian INOVA2 500 MHz spectrometers. Chemical shifts are reported in δ (ppm). For ^1H and ^{13}C NMR spectra, the residual solvent peaks were used as an internal reference. Molecular weight, radius of gyration, and polydispersity were determined by size exclusion chromatography (SEC) in dimethylacetamide (DMAc) with 50 mM LiCl at 50 °C and a flow rate of 1.0 mL/min (Agilent isocratic pump, degasser, and auto-sampler, columns: PLgel 5 μm guard + two ViscoGel I-series G3078 mixed bed columns: molecular weight range 0-20 × 10^3 and 0-100 × 10^4 g mol^{-1}). Detection consisted of a Wyatt Optilab T-rEX refractive index detector operating at 658 nm and a Wyatt miniDAWN Treos light scattering detector operating at 659 nm. Absolute molecular weights and polydispersities were calculated using Wyatt ASTRA software.

Synthesis and NMR characterization of complex 4

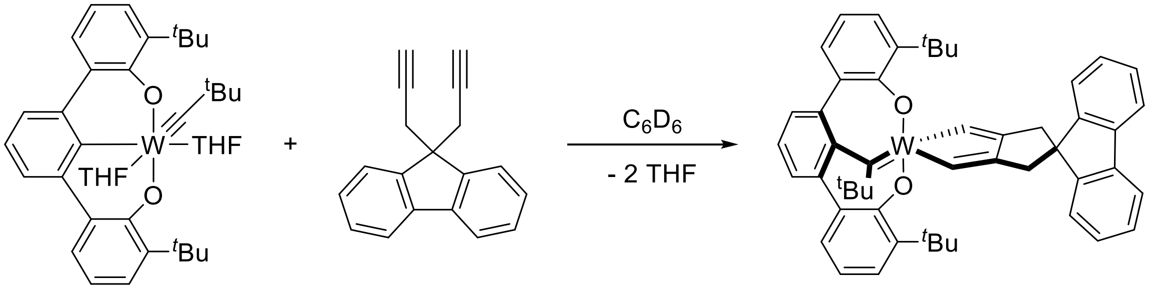

3 **4**

A 20 mL vial equipped with a stir bar was charged with compound **3** (10 mg, 12.9 μmol) and dissolved in minimal (< 1 mL) benzene. An aliquot of dipropargylfluorene (3.2 mg, 12.9 μmol) from a stock solution in benzene was added via a micropipette. The solution immediately changed color from orange/brown to dark purple upon addition of the dipropargylfluorene. Complex **4** forms rapidly upon addition. Since complex **4** decomposes upon introduction of vacuum it was not isolated. ^1H NMR (500

MHz, C_7D_8, δ (ppm)): 8.75 (s, 1H, H50), 8.63 (s, 1H, H32), 7.50 (d, $^{2}J_{HH}$ = 7.0 Hz, 8.4 Hz, 2H, H8/H10), 7.51 (d, $^{2}J_{HH}$ = 8.1 Hz 2H, H40/H43), 7.43 (d, $^{2}J_{HH}$ = 7.8 Hz 2H, H37/H46), 7.35, (dd, $^{2}J_{HH}$ = 8.1 Hz, 1.6 Hz, 2H, H3/H16), 7.28 (t, $^{2}J_{HH}$ = 7.6 Hz, 1H, H9), 7.15 (t, $^{2}J_{HH}$ = 7.8 Hz, 2H, H39/H44), 7.14 (dd, $^{2}J_{HH}$ = 7.6 Hz, 0.9 Hz, 2H, H5/H14), 7.06 (td, $^{2}J_{HH}$ = 7.3 Hz, 1.1 Hz, 2H, H38/H45), 6.80 (t, $^{2}J_{HH}$ = 7.7 Hz, 2H, H4/H15), 2.85 (s, 2H, H48), 2.71 (s, 2H, H34), 1.56 (s, 18H, H20-22/H24-26), 0.88 (s, 9H, H29-31). ^{13}C NMR: 305.7 (C27), 188.9 (C32), 188.1 (C50), 168.3 (C1/C18), 159.0 (C7/C11), 150.1 (C36/C47), 140.1 (C41/C42), 138.3 (C2/C17), 134.9 (C9), 134.2 (C8/C10), 130.7 (C6/C13), 130.2 (C49), 129.2 (C5/C14), 128.4 (C33), 127.7 (C38/C45), 127.5 (C39/C44), 126.4 (C3/C16), 122.9 (C37/C46), 119.9 (C40/C43), 119.3 (C4/C15), 102.3 (C12), 51.2 (C48), 50.7 (C35), 48.6 (C34), 46.9 (C28), 35.6 (C19/C23), 35.0 (C29-31), 29.9 (C20-22/C24-26).

Table S1. ^{1}H and ^{13}C NMR chemical shifts for complex **4** (toluene-d_8).

Position	δ^{1}H (ppm)	δ^{13}C (ppm)
1, 18	-	168.3
2, 17	-	138.3
3, 16	7.35	126.4
4, 15	6.80	119.3
5, 14	7.14	129.2
6, 13	-	130.7
7, 11	-	159.0
8, 10	7.50	134.2
9	7.28	134.9
12	-	102.3
19, 23	-	35.6
20-22, 24-26	1.56	29.9
27	-	305.7
28	-	46.9
29-31	0.88	35.0
32	8.63	188.9
33	-	128.4
34	2.71	48.6
35	-	50.7
36, 47	-	150.1
37, 46	7.43	122.9
38, 45	7.06	127.7
39, 44	7.15	127.5
40, 43	7.51	119.9
41, 42	-	140.1
48	2.85	51.2
49	-	130.2
50	8.75	188.1

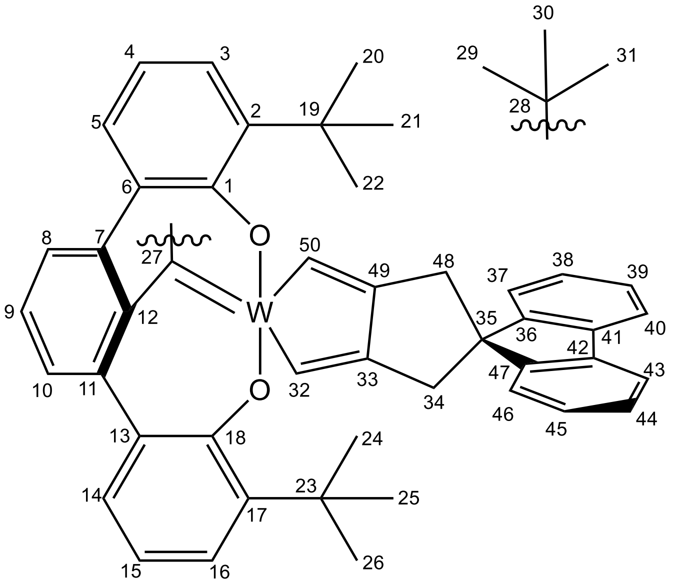

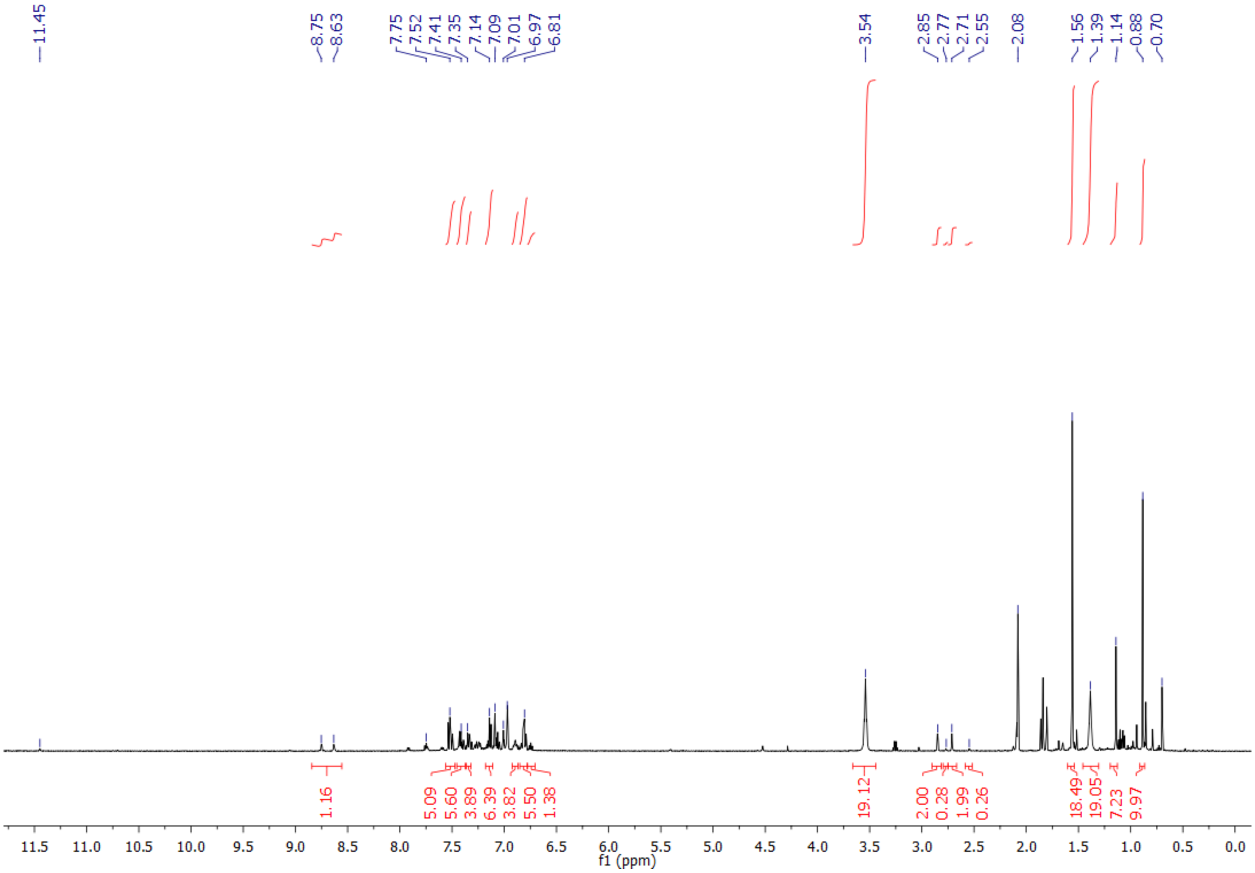

Figure S1. ^{1}H NMR spectrum of **4** (Toluene-d_8, 500 MHz, 25 °C).

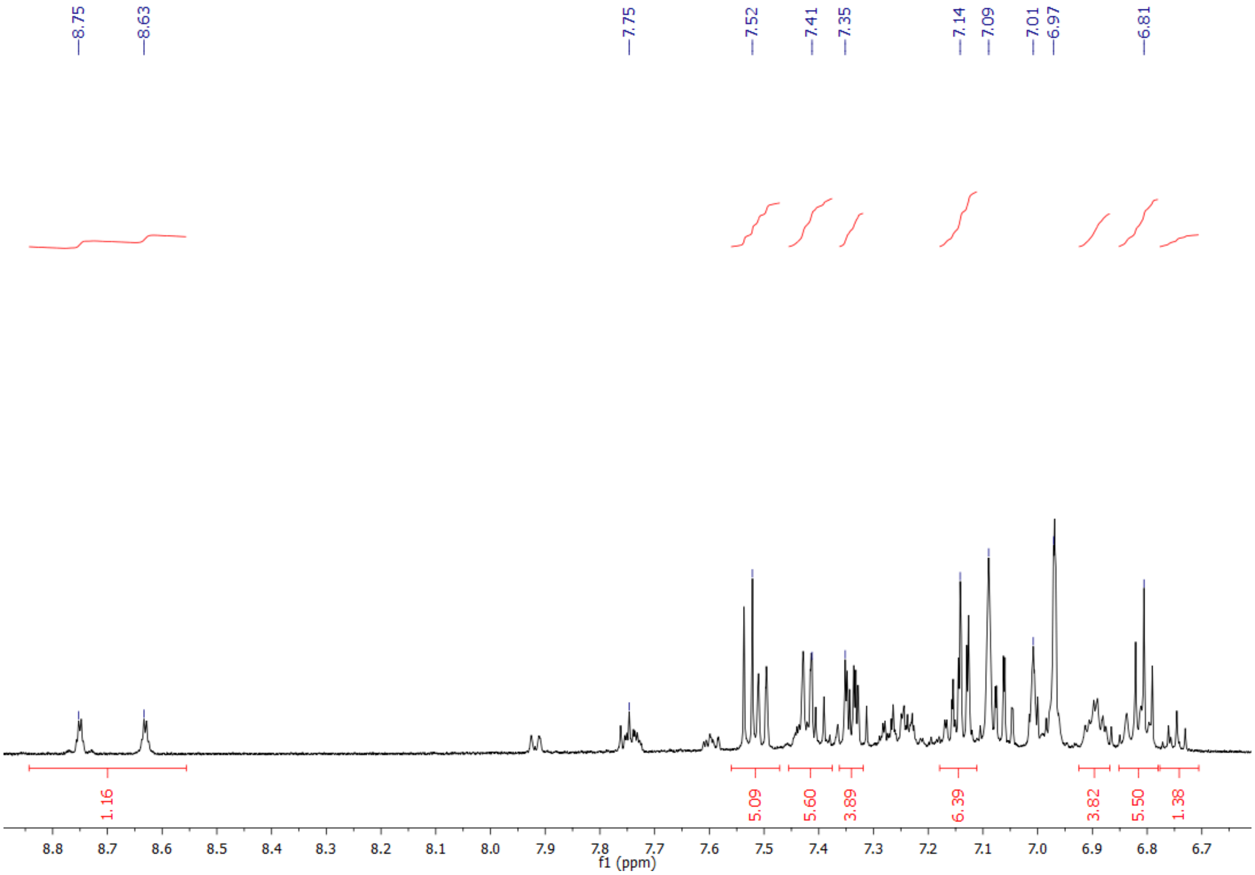

Figure S2. ^{1}H NMR spectrum of **4**, expansion of aromatic region

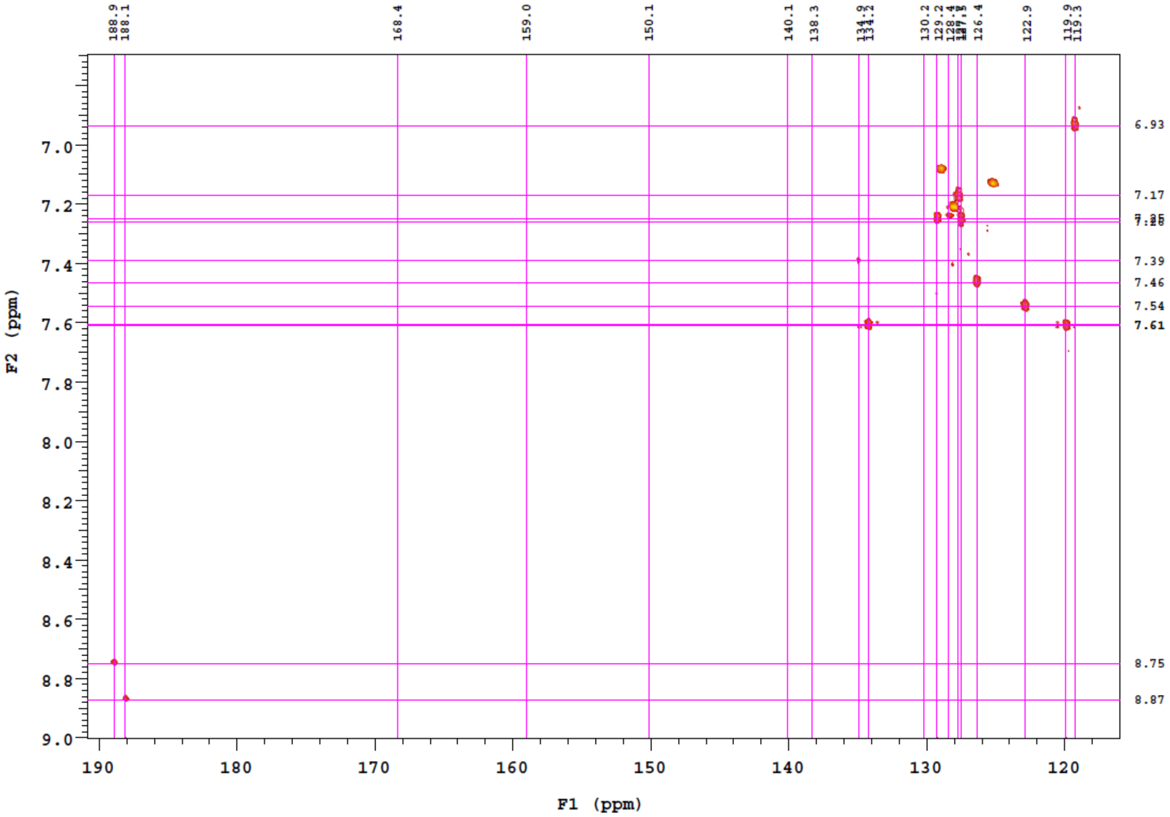

Figure S3. ^{1}H-^{13}C gHSQC NMR spectrum of **4** expansion of aromatic region (Toluene-d_8, 500 MHz, 0 °C).

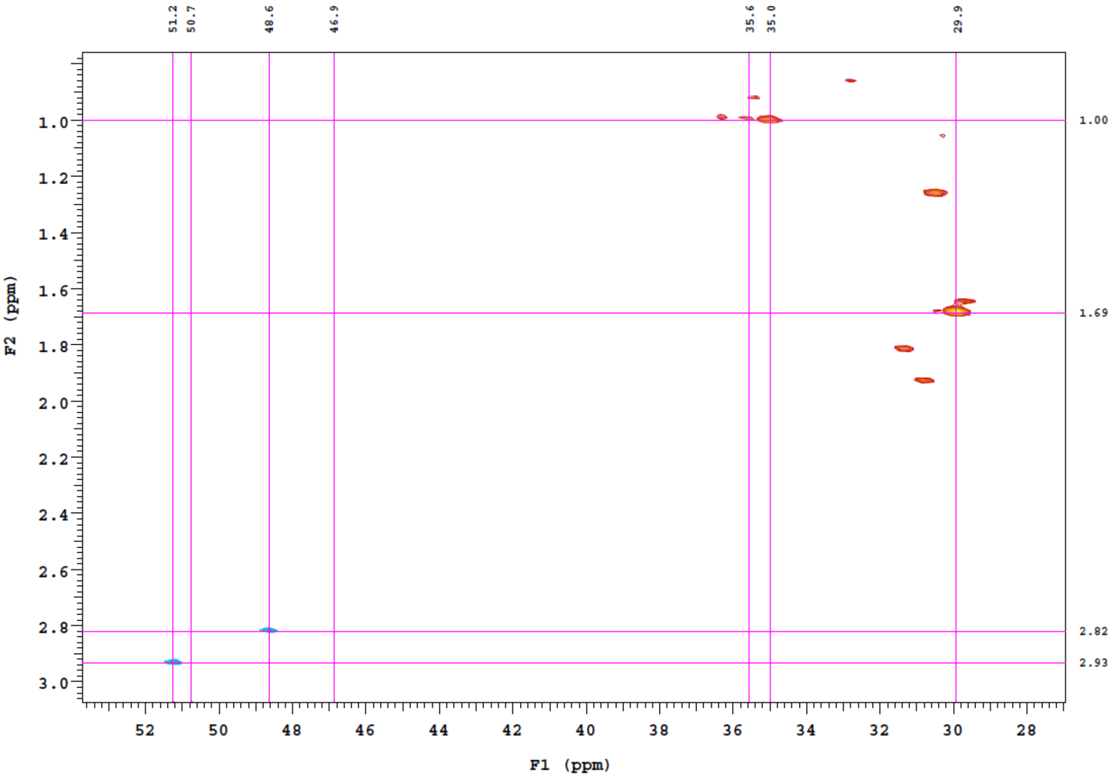

Figure S4. ^{1}H-^{13}C gHSQC NMR spectrum of **4**, expansion of aliphatic region (Toluene-d_8, 500 MHz, 0 °C).

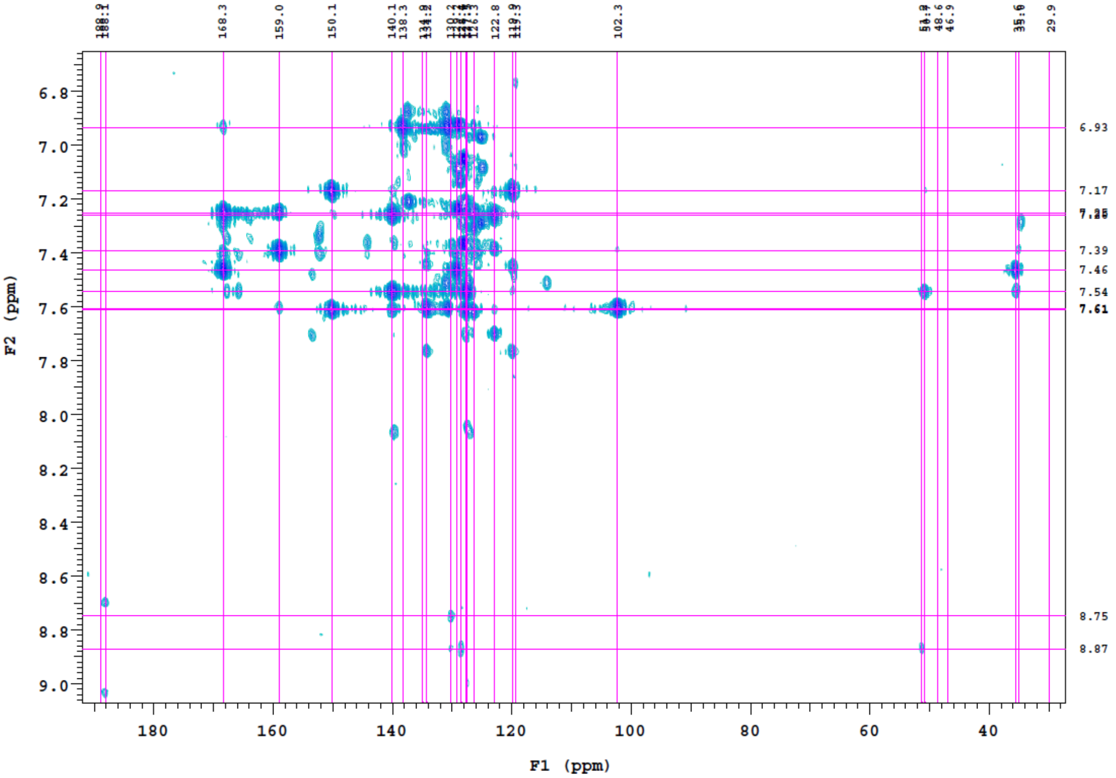

Figure S5. ^{1}H-^{13}C gHMBC spectrum **4**, expansion of aromatic region.

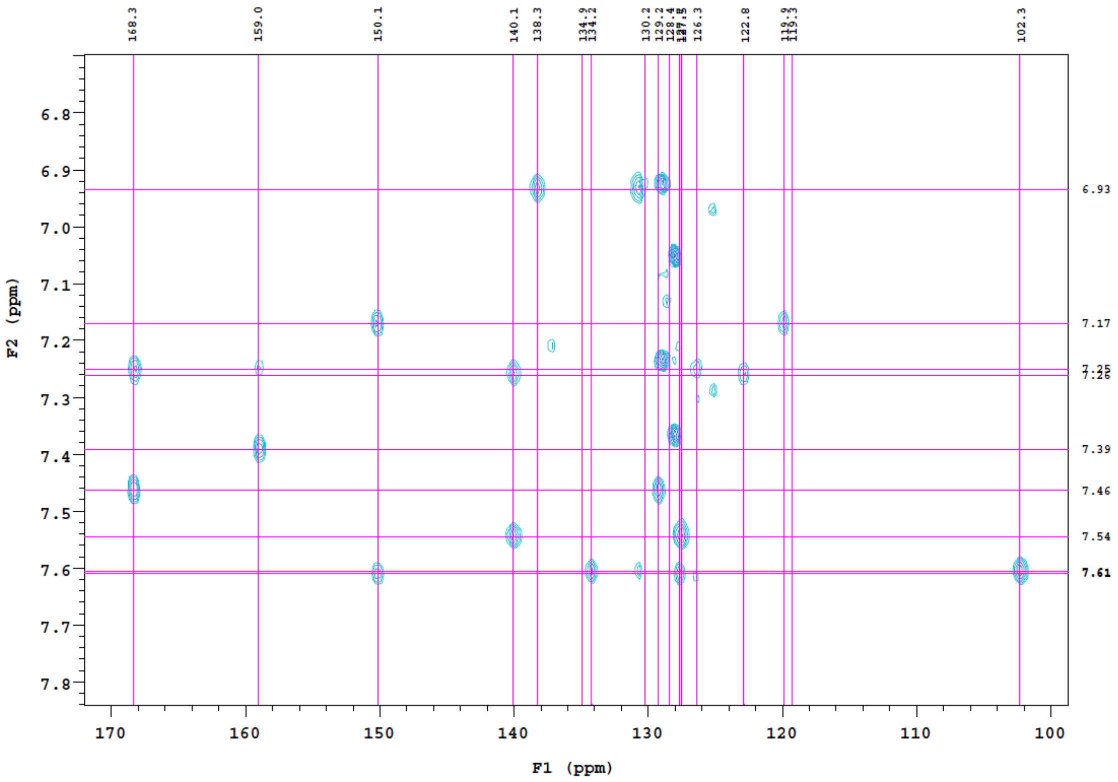

Figure S6. ^{1}H-^{13}C gHMBC spectrum of **4**, expansion of aromatic region.

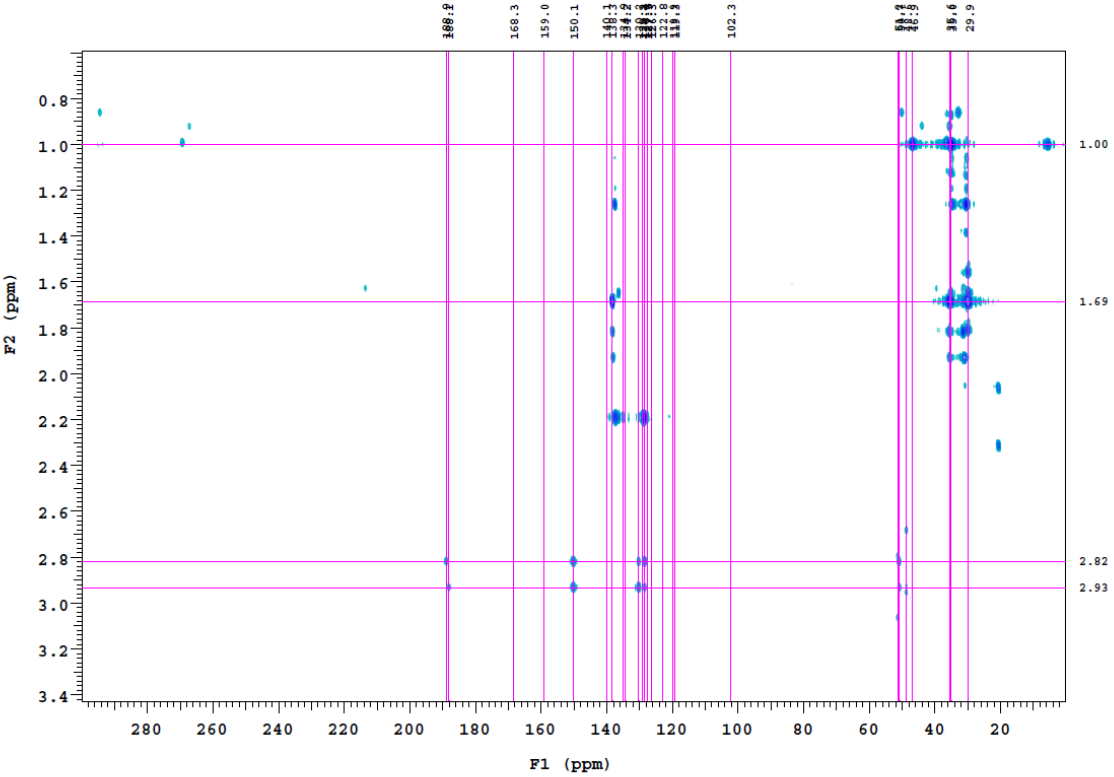

Figure S7. ^{1}H-^{13}C gHMBC spectrum of **4**, expansion of aliphatic region.

nOe Data

Table S2. Calculated distances vs. average in model for complex **4**

4			
protons[a]	normal nOe[b]	average calculated distance (Å)[c]	nOe distance (Å)[d]
1.57 - 7.35	8.57	2.87	*ref. dist.*
1.57 - 8.75	1.05	4.13	4.07
1.57 - 7.43	1.81	3.31	3.72
1.57 - 7.06	0.62	4.23	4.45
1.57 - 0.88	0.26	5.12	5.14
8.75 - 2.85	2.71	2.93	*ref. dist.*
8.75 - 1.57	0.61	4.13	3.76

The average calculated distance is based on the DFT model shown in Figure S28

[a] the first chemical shift indicates the proton which was selectively inverted in a NOESY1D experiment, and the second the proton at which the nOe was measured.

[b] normalized nOe, *e.g.* for a methyl group the value of the integral divided by 3.

[c] average calculated distance, e.g. between proton **a** and protons **b-d** in a methyl group, $r_{a,b\text{-}d} = ((r_{ab}^{-6} + r_{ac}^{-6} + r_{ad}^{-6})/3)^{-1/6}$ where r_{ab}, r_{ac} and r_{ad} are read on the geometry calculated by DFT.

[d] distance calculated from nOes, using a reference distance (*ref. dist*. below): nOe dist. = *ref. dist*. X $(\text{nOe}/\text{ref.nOe})^{-1/6}$

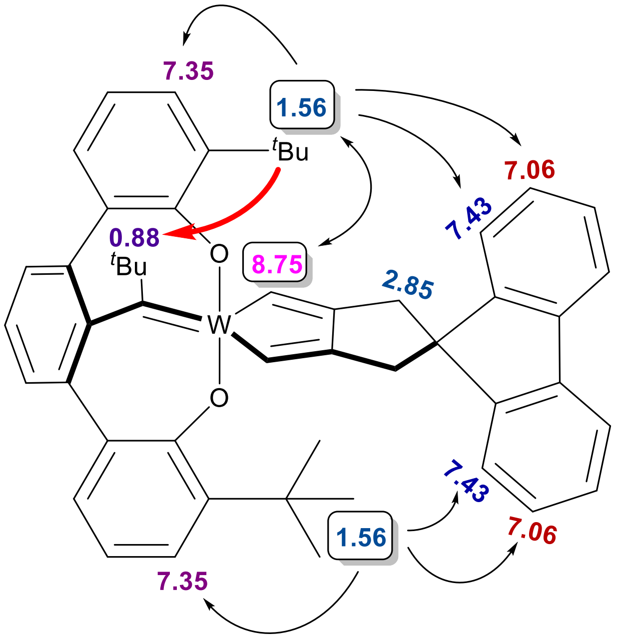

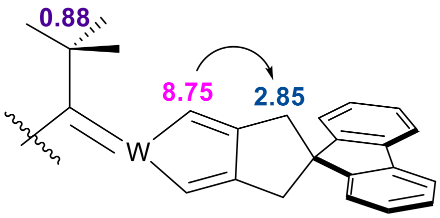

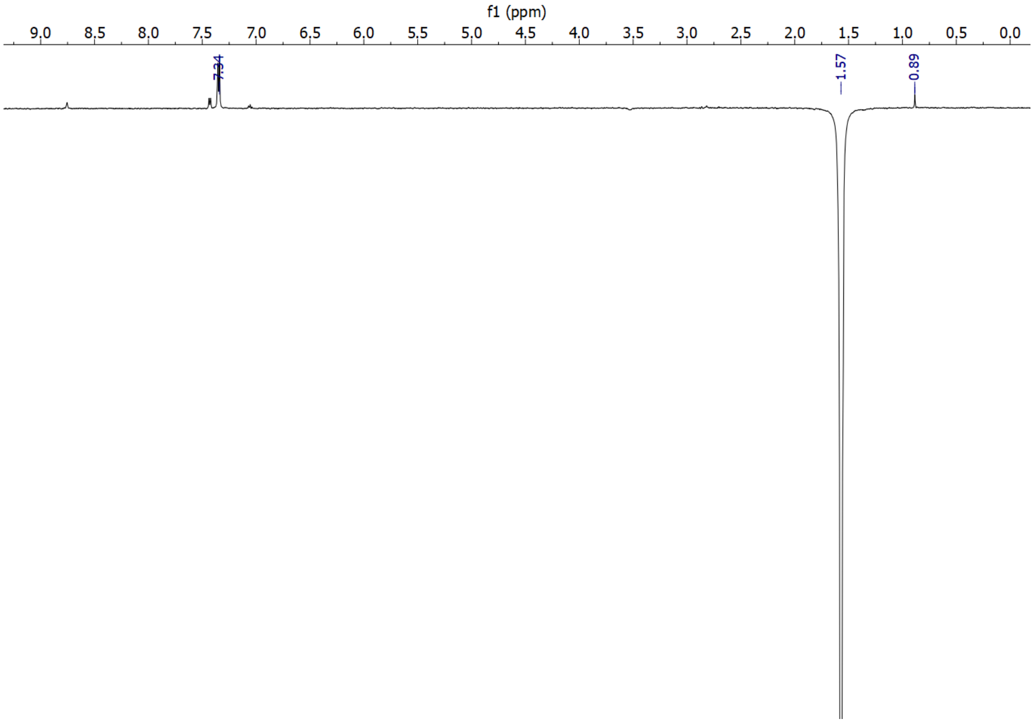

Figure S8. ^{1}H NOE experiment inverting 1.57 ppm (ligand ^{t}Bu: H20-22, H24-26) showing coupling through space to 0.88 (H29-31), 7.06 (H38/45), 7.35 (H3/16), 7.43 (H37/46), and 8.75 (H50) ppm (the dipropargylfluorene backbone).

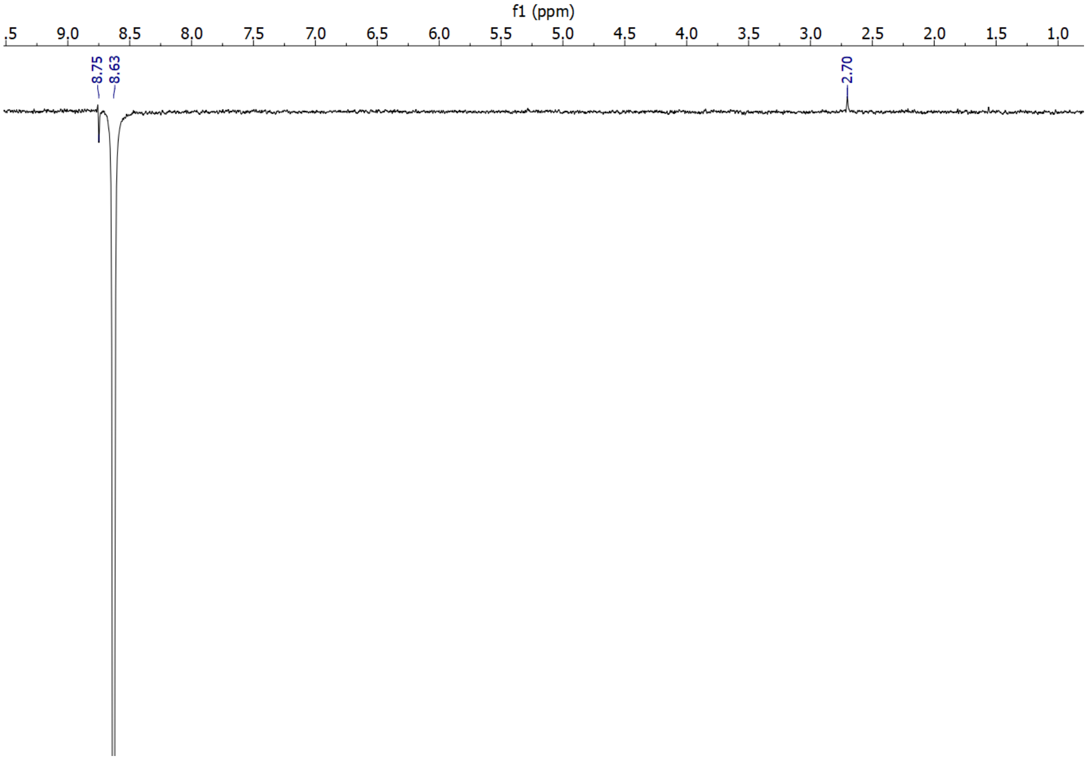

Figure S9. ^{1}H NOE experiment inverting 8.63 ppm (α carbon of metallacylopentadiene, H32) showing coupling to the dipropargylfluorene backbone (2.70 ppm, H34).

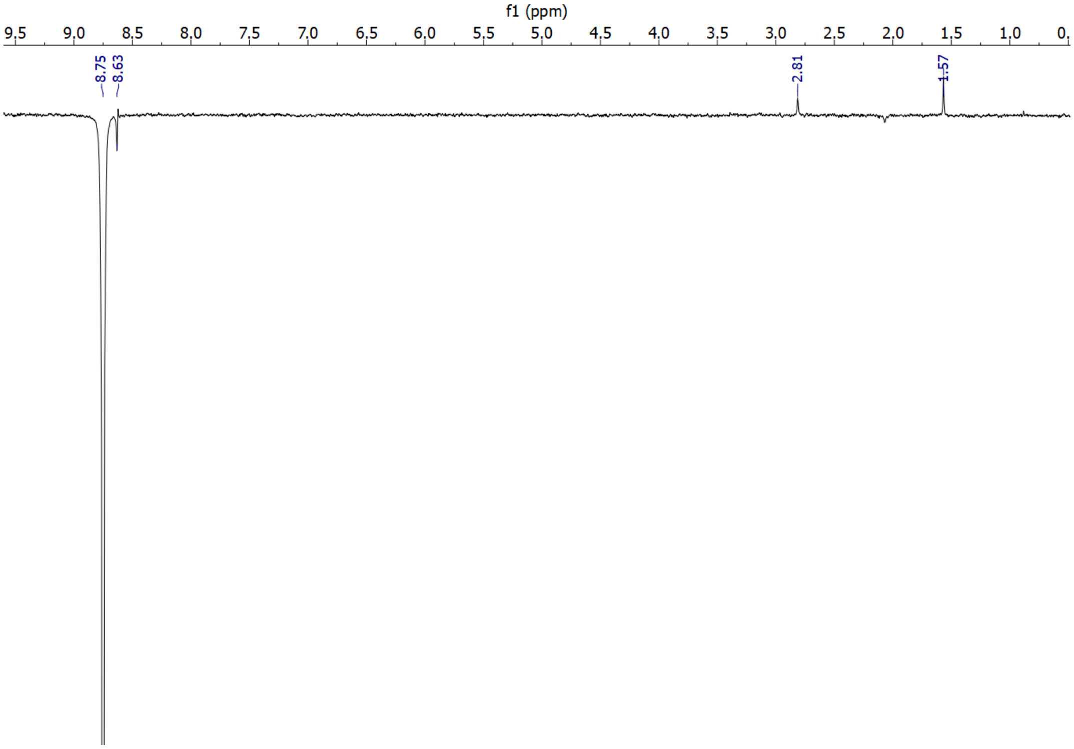

Figure S10. ^{1}H NOE experiment inverting 8.75 ppm (other α carbon of metallacylopentadiene, H50) showing coupling to the dipropargylfluorene backbone (2.81 ppm, H48) and also ligand ^{t}Bu groups (1.57 ppm, H20-22, 24-26).

Preparation of the equilibrium mixture 4/4-THF

A 20 mL vial equipped with a stir bar was charged with compound **3** (10 mg, 12.9 µmol) and dissolved in minimal (< 1 mL) benzene. An aliquot of dipropargylfluorene (3.2 mg, 12.9 µmol) from a stock solution in benzene was added via micropipette. The solution immediately changed color from orange/brown to dark purple upon addition of the dipropargylfluorene. The reaction approaches equilibrium after 5 h. ^{1}H NMR (500 MHz, C_7D_8, δ (ppm)): 9.05 (s, 1H, H50), 7.92 (d, $^{2}J_{HH}$ = 7.3 Hz, 2H, H37/H46), 7.73 (s, 1H, H32), 7.58 (d, $^{2}J_{HH}$ = 7.3 Hz, 2H, H40/H43), 7.42 (dd, $^{2}J_{HH}$ = 8.7 Hz, 2.1 Hz, 2H, H3/H16), 7.41 (d, $^{2}J_{HH}$ = 7.3 Hz, 2H, H8/H10), 7.35 (td, $^{2}J_{HH}$ = 7.3 Hz, 0.9 Hz, 2H, H38/H45), 7.24 (dd, $^{2}J_{HH}$ = 7.6 Hz, 1.7 Hz, 2H, H39/H44), 7.24 (dd, $^{2}J_{HH}$ = 7.6 Hz, 1.7 Hz, 2H, H5/H14), 7.17 (t, $^{2}J_{HH}$ = 7.6 Hz, 1H, H9), 6.88 (t, $^{2}J_{HH}$ = 7.5 Hz, 2H, H4/H15), 2.77 (d, $^{2}J_{HH}$ = 1.2 Hz, 2H, H48), 2.54 (d, $^{2}J_{HH}$ = 1.2 Hz, 2H, H34), 1.80 (s, 18H, H20-22/H24-26), 0.79 (s, 9H, H29-31). ^{13}C NMR: 267.1 (C27), 175.8 (C32), 177.3 (C49), 179.6 (C50), 167.6 (C18/C1), 163.7 (C7/C11), 159.4 (C33) 153.4 (C36/C47), 139.6 (C41/C42), 138.0 (C2/C17) 131.0 (C8/C10), 135.0 (C9), 127.8 (C5/C14), 127.5 (C38/C45), 127.0 (C39/C44), 127.0 (C3/C16), 123.8 (C37/C46), 120.2 (C4/C15), 119.6 (C40/C43), 114.1 (C12), 58.4 (C35), 44.1 (C48), 44.0 (C28), 42.7 (C34), 35.4 (C19/C23), 35.4 (C29-C31), 30.7 (C20-22 and C24-26).

Table S3. ^{1}H and ^{13}C NMR chemical shifts for complex **4-THF**

Position	δ^{1}H (ppm)	δ^{13}C (ppm)
1, 18	-	167.6
2, 17	-	138.0
3, 16	7.42	127.0
4, 15	6.88	120.2
5, 14	7.24	127.8
6, 13	-	131.0
7, 11	-	163.7
8, 10	7.41	131.0
9	7.17	135.0
12	-	114.1
19, 23	-	35.4
20-22, 24-26	1.80	30.7
27	-	267.1
28	-	44.0
29-31	0.79	35.4
32	7.73	175.8
33	-	159.4
34	2.77	42.7
35	-	58.4
36, 47	-	153.4
37, 46	7.92	123.8
38, 45	7.35	127.5
39, 44	7.24	127.0
40, 43	7.58	119.6
41, 42	-	139.6
48	2.54	44.1
49	-	177.3
50	9.05	179.6

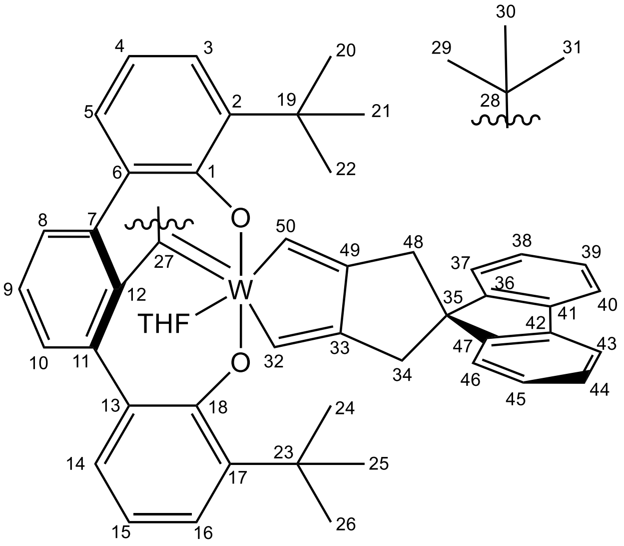

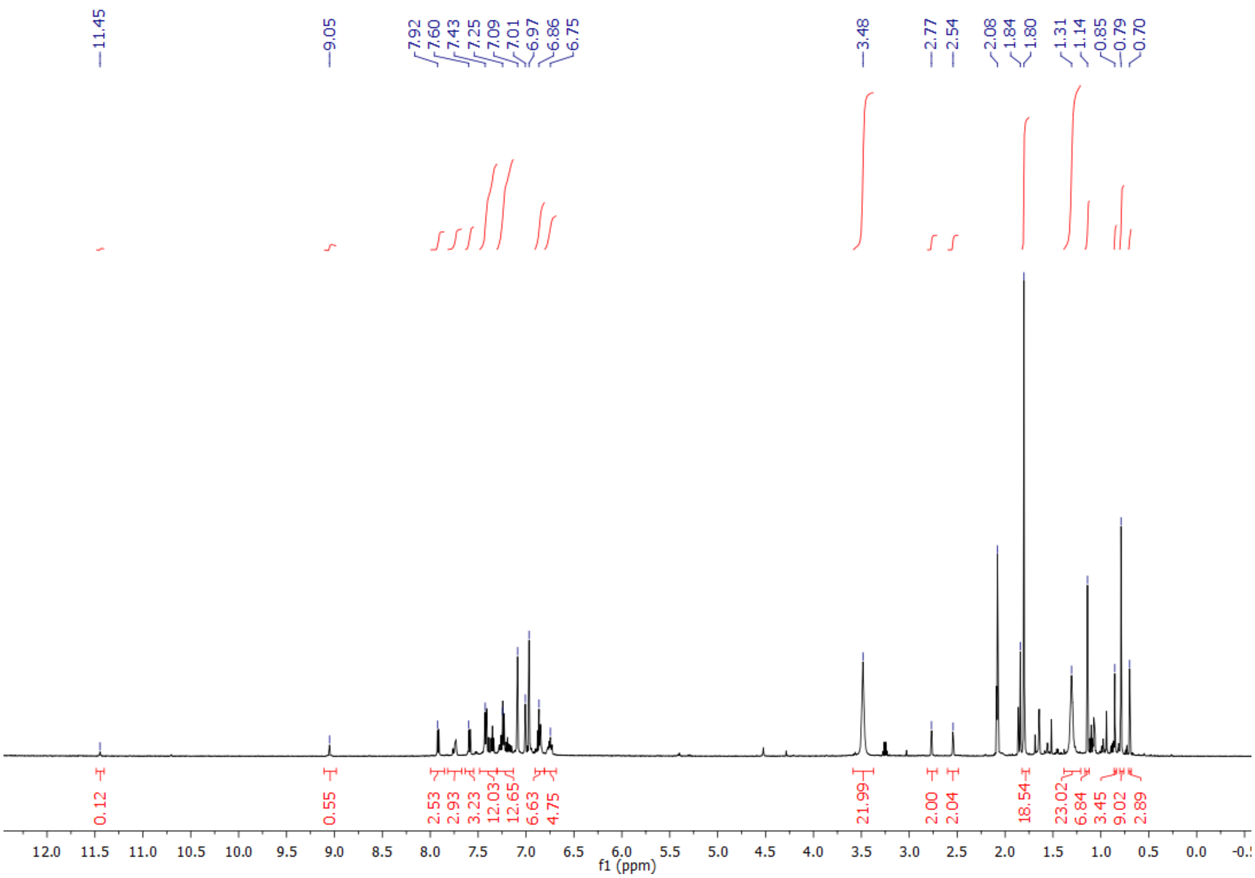

Figure S11. ^{1}H NMR spectrum of **4-THF** (Toluene-d_8, 500 MHz, 25 °C)

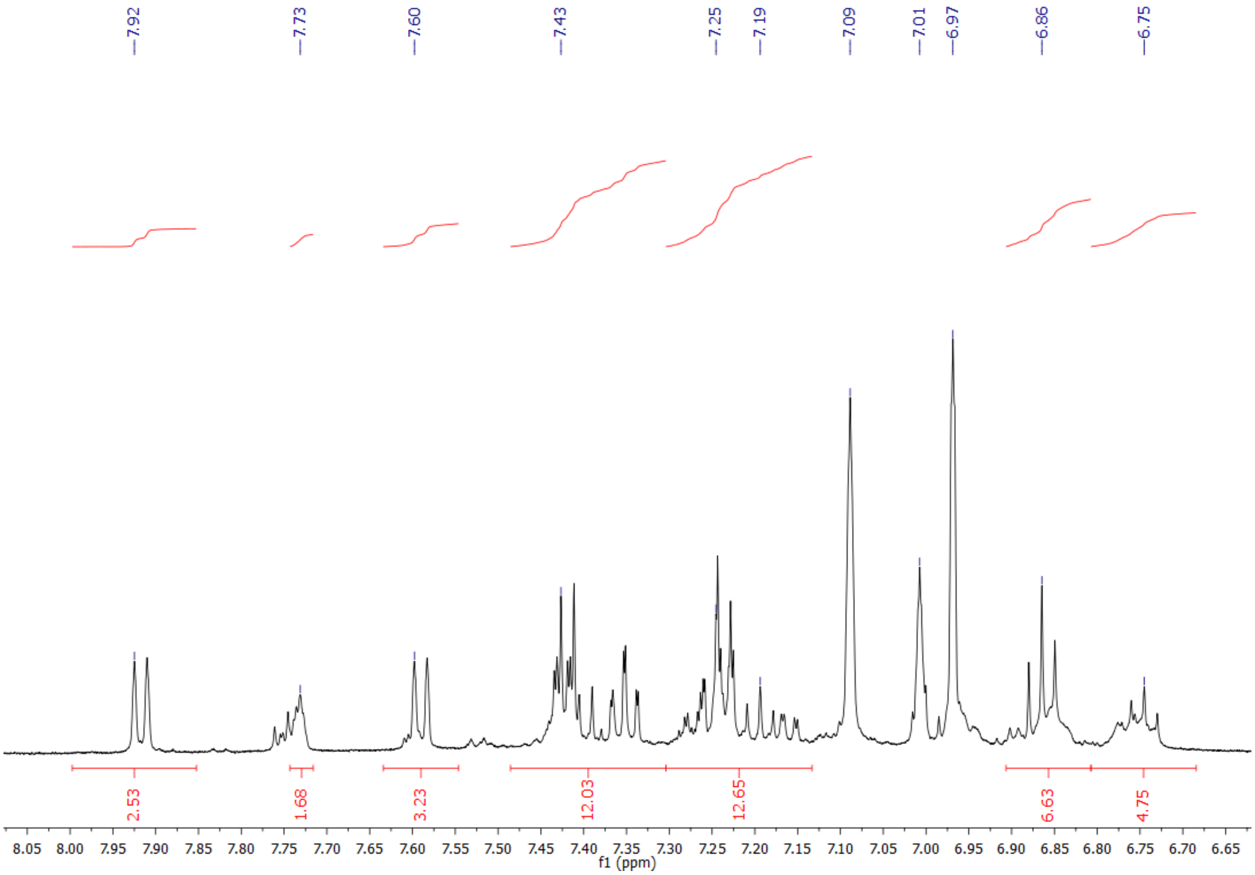

Figure S12. ^{1}H NMR spectrum of **4-THF** expansion of aromatic region.

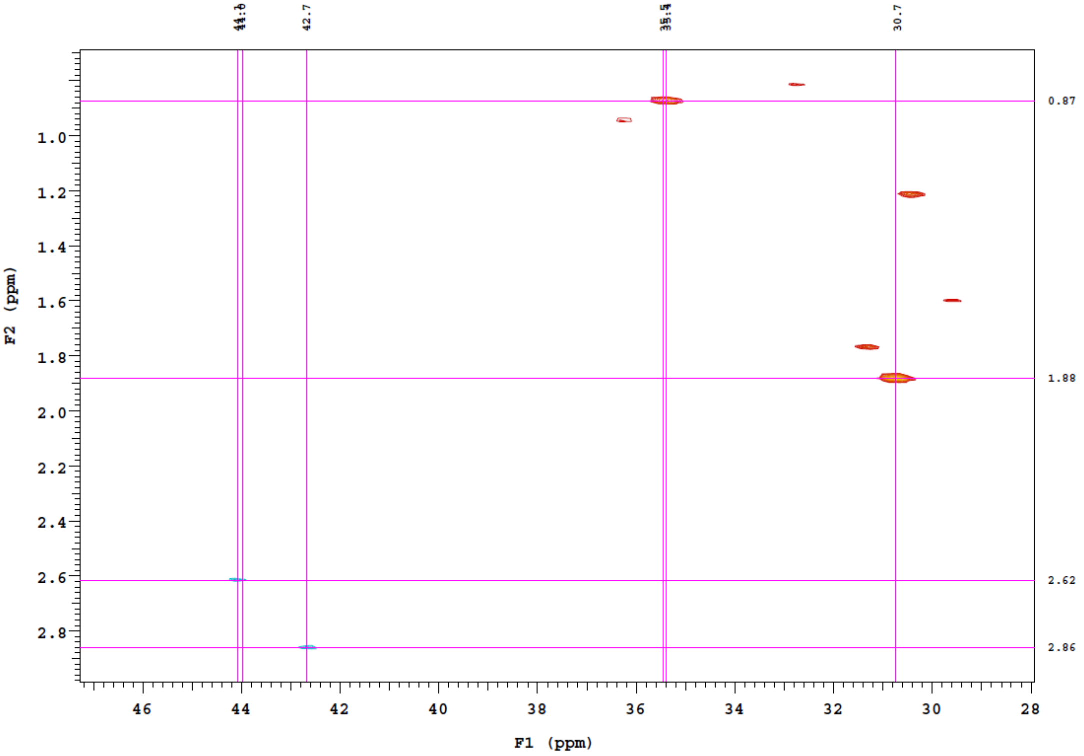

Figure S13. ^1H-^{13}C gHSQC NMR spectrum of **4-THF**, expansion of the aliphatic region

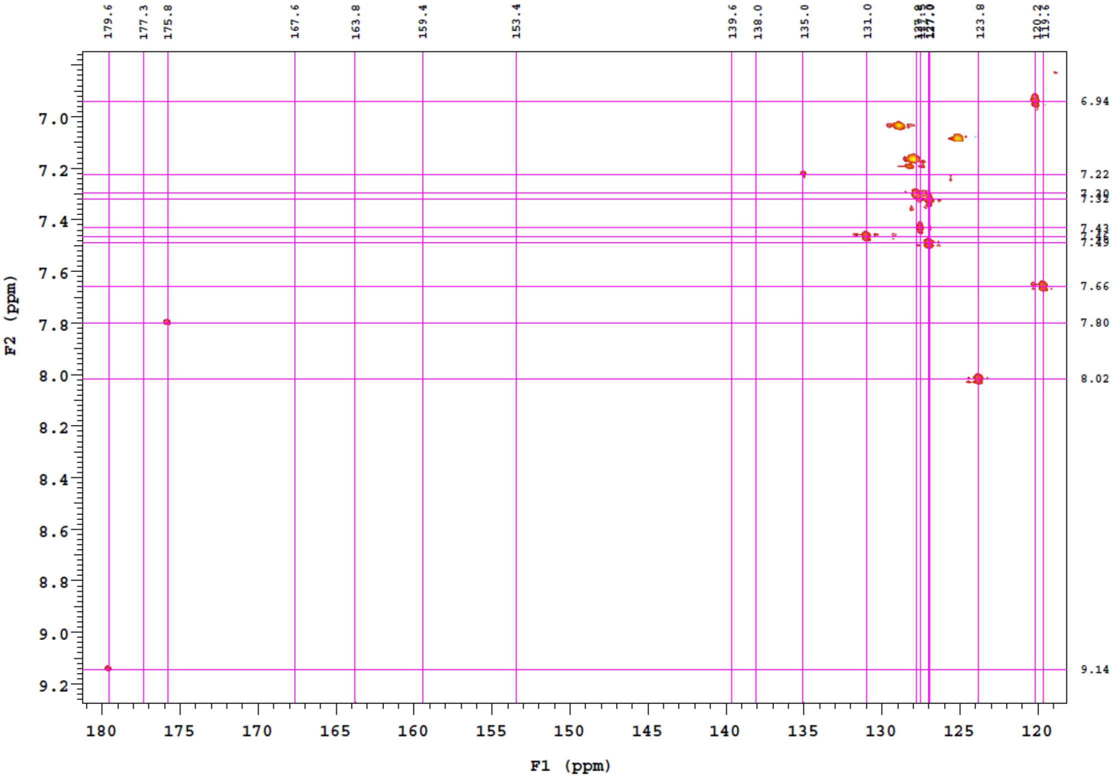

Figure S14. ^{1}H-^{13}C gHSQC NMR spectrum of **4-THF**, expansion of the aromatic region

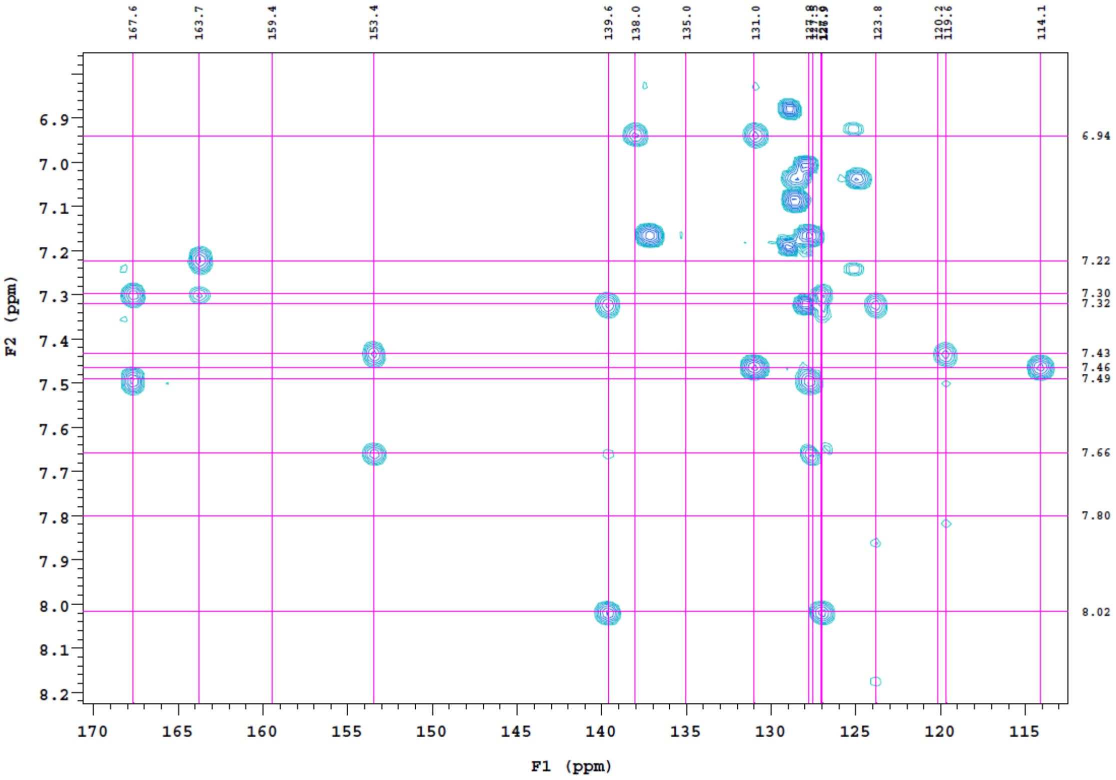

Figure S15. ^{1}H-^{13}C gHMBC NMR spectrum of **4-THF**, expansion of the aromatic region

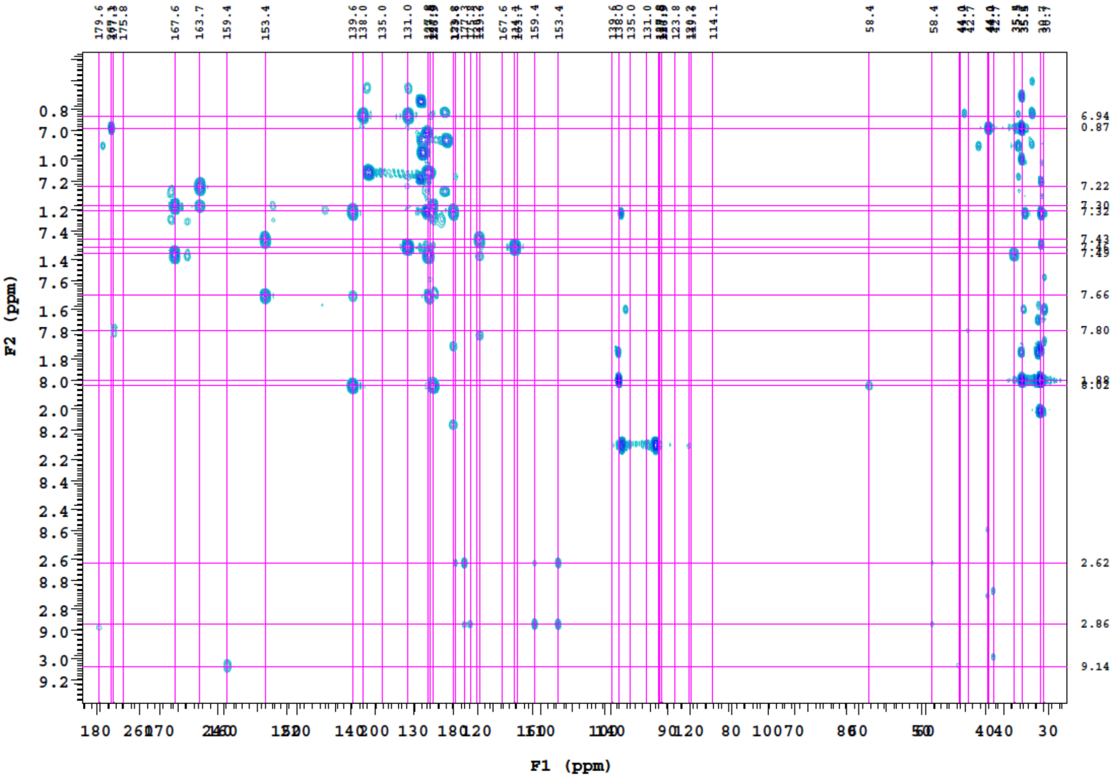

Figure S16. ^{1}H-^{13}C gHMBC NMR spectrum of **4-THF**, expansion of the aromatic region

nOe Data

Table S4. Calculated distances vs. average in model for complex **4-THF**

4-THF			
protons[a]	normal nOe[b]	average calculated distance (Å)[c]	nOe distance (Å)[d]
7.73 - 2.77	2.57	3.00	*ref. dist.*
7.73 - 1.80	0.42		4.06
9.05 - 2.54	3.76	3.00	*ref. dist.*
9.05 - 1.80	0.50		4.19
9.05 - 0.79	7.40	2.52	2.68

The average calculated distance is based on the DFT model shown in Figure S29

[a] the first chemical shift indicates the proton which was selectively inverted in a NOESY1D experiment, and the second the proton at which the nOe was measured.

[b] normalized nOe, *e.g*. for a methyl group the value of the integral divided by 3.

[c] average calculated distance, e.g. between proton **a** and protons **b-d** in a methyl group, $r_{a,b\text{-}d} = ((r_{ab}^{-6} + r_{ac}^{-6} + r_{ad}^{-6})/3)^{-1/6}$ where r_{ab}, r_{ac} and r_{ad} are read on the geometry calculated by DFT.

[d] distance calculated from nOes, using a reference distance (*ref. dist*. below): nOe dist. = *ref. dist*. X $(\text{nOe/ref.nOe})^{-1/6}$

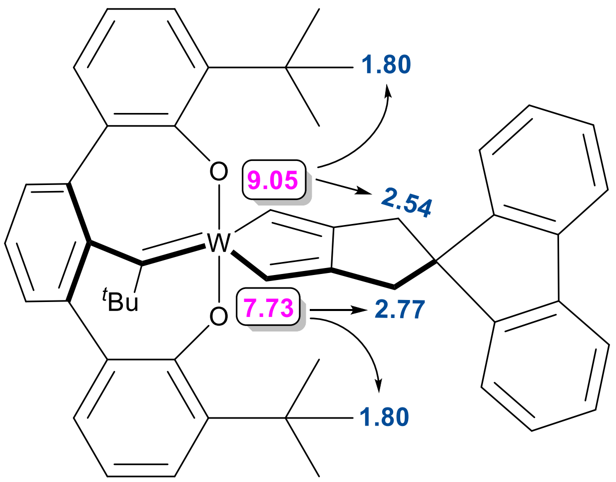

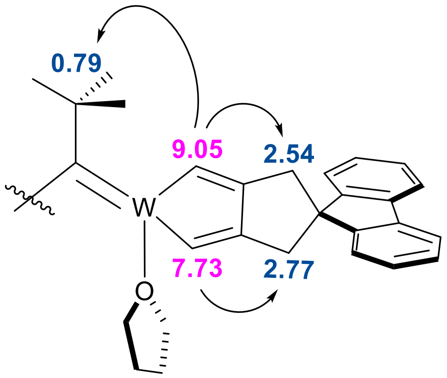

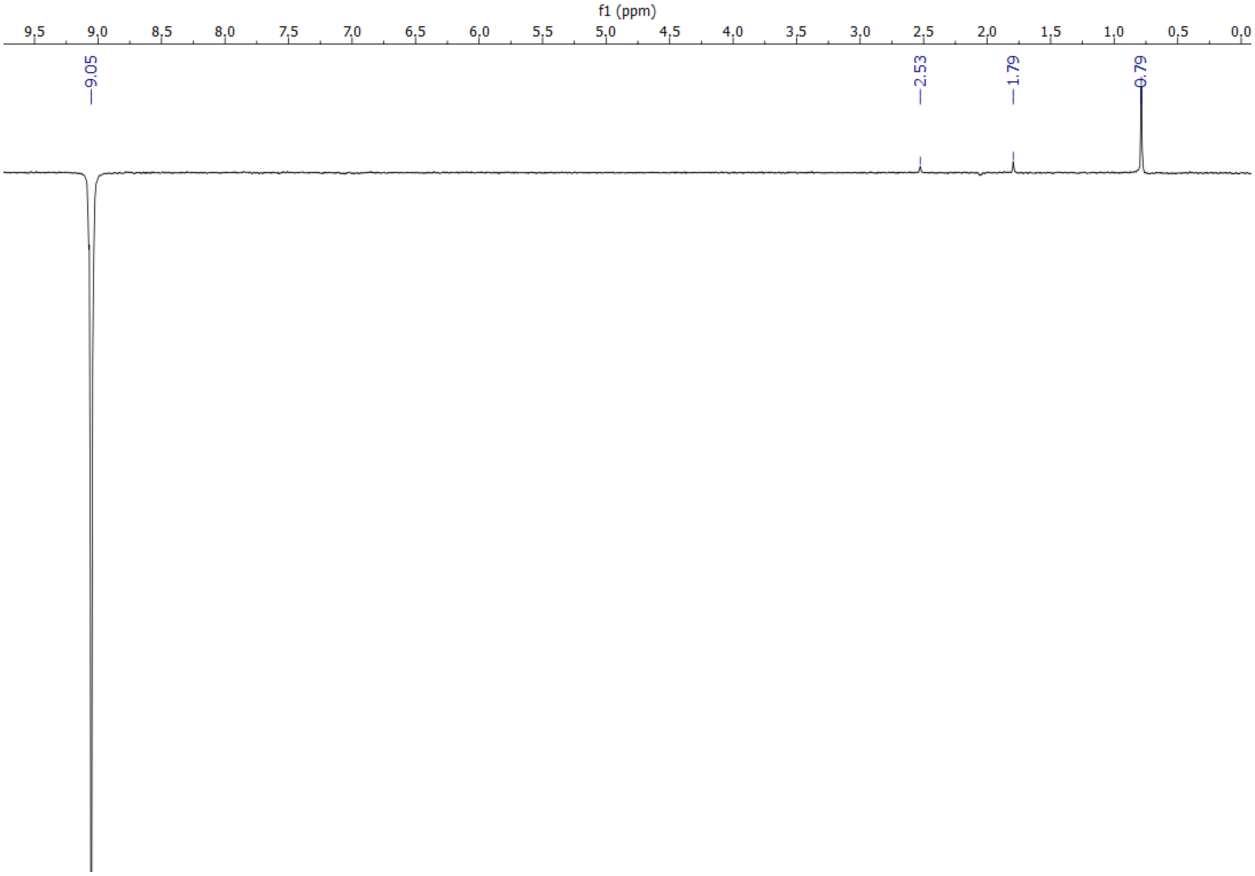

Figure S17. ^{1}H NOE experiment inverting 9.05 ppm (α carbon of metallacylopentadiene) showing coupling to the ^{t}Bu protons on the alkylidene (0.79 ppm, H29-31) and 2.53 (H48), 1.79 (H20-22, 24-26) ppm.

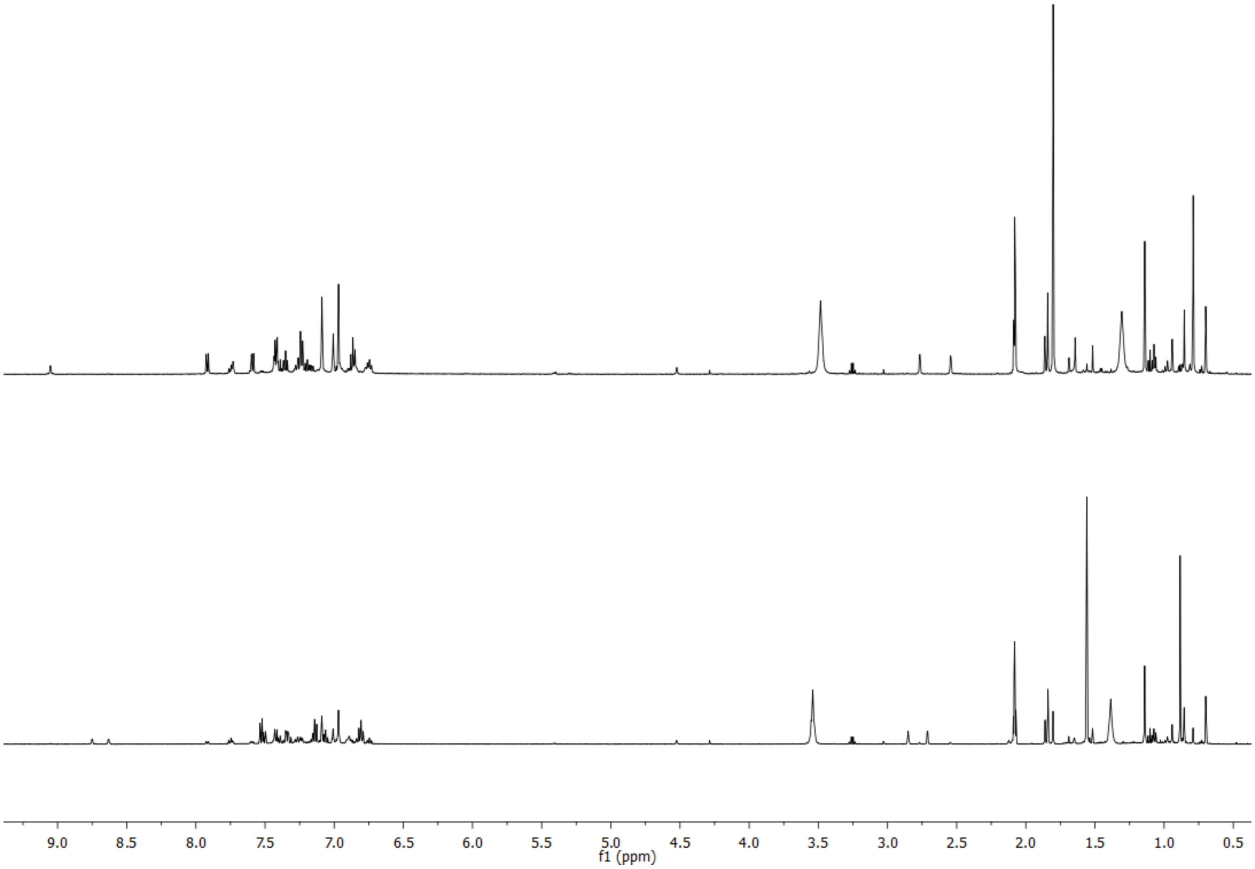

Figure S18. ^{1}H NMR comparison of initial product **4** (bottom) to **4-THF** (above)

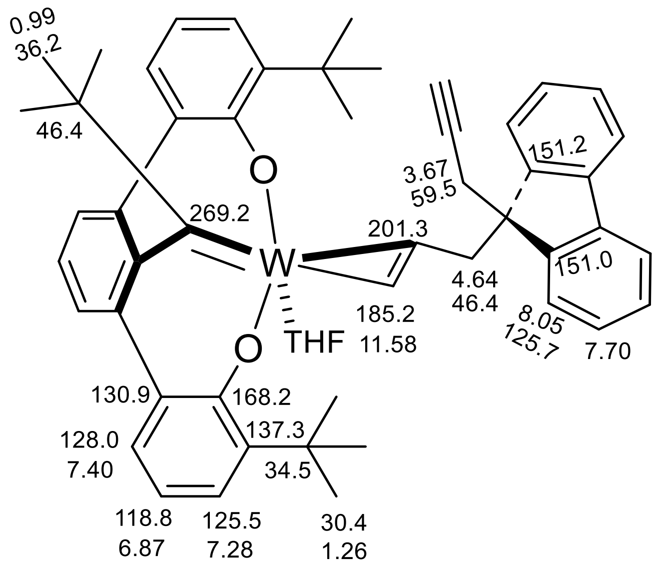

Figure S19. ^{1}H NMR chemical shifts for the tentatively assigned minor impurity with the metallacyclopropene in the *syn*-configuration.

Kinetics for the conversion of 4 to 4-THF

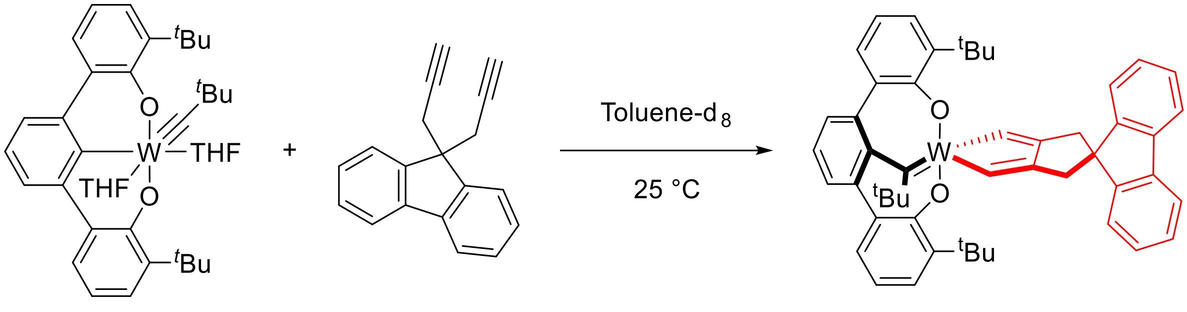

1 **4**

In a nitrogen filled glovebox, a J-Young NMR tube was charged with 300 µL stock solution (0.0333 g/mL in toluene-*d*$_8$) of complex **1** (0.0100 g, 0.0130 mmol). A 400 µL dipropargylfluorene solution (3.2 mg, 0.0130 mmol, 0.0080 g/mL) was added dropwise into the J-Young tube while shaking the tube. The initial concentration of **1** was 1.857 x 10^{-2} M. Then the tube was taken out of the glovebox for NMR experiments. The NMR spectra were taken at desired time points.

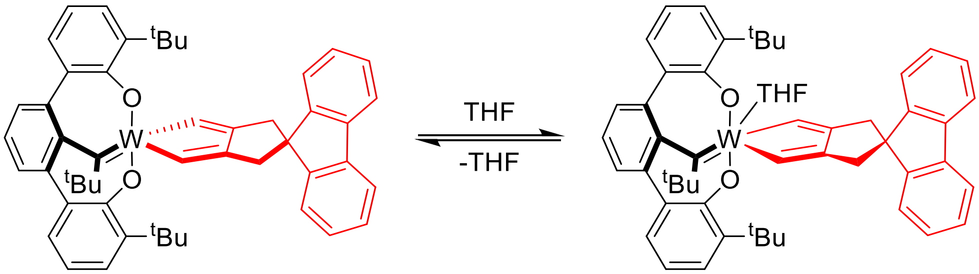

4 **4-THF**

Method

The conversion of **4** to **4-THF** was studied by NMR spectroscopy by tracking the methylene (CH_2) groups on the propargyl arms of the fluorene substituent on **4-THF**, which resonate at 2.54 and 2.77 ppm. The methylene units on **4** show up as doublets at 2.71 ppm and 2.85 ppm. (Figure S20)

Results

Integration of the methylene resonances and plotting using the equation $ln\frac{[\mathbf{4}]}{[\mathbf{4}]_0} = -kt$ provides the rate constant (k) for the conversion of **4** to **4**-THF versus time. Using this method, a rate constant of 1.41 (±0.04) x 10^{-4} s^{-1} was obtained for the conversion of **4** to **4-THF**. To investigate if tetrahydrofuran (THF) assists the formation of complex **4-THF**, another kinetics study with 10-fold excess of THF (with reference to **1**) was set up; the rate of the reaction was determined to be 1.64(±0.15) x 10^{-4} s^{-1} shown in Figure S20.

The similar rate constants indicate the reaction is zero order in THF. However, this result cannot rule out the rapid association and dissociation of THF on complex **4** prior to rate-determining ligand reorganization.

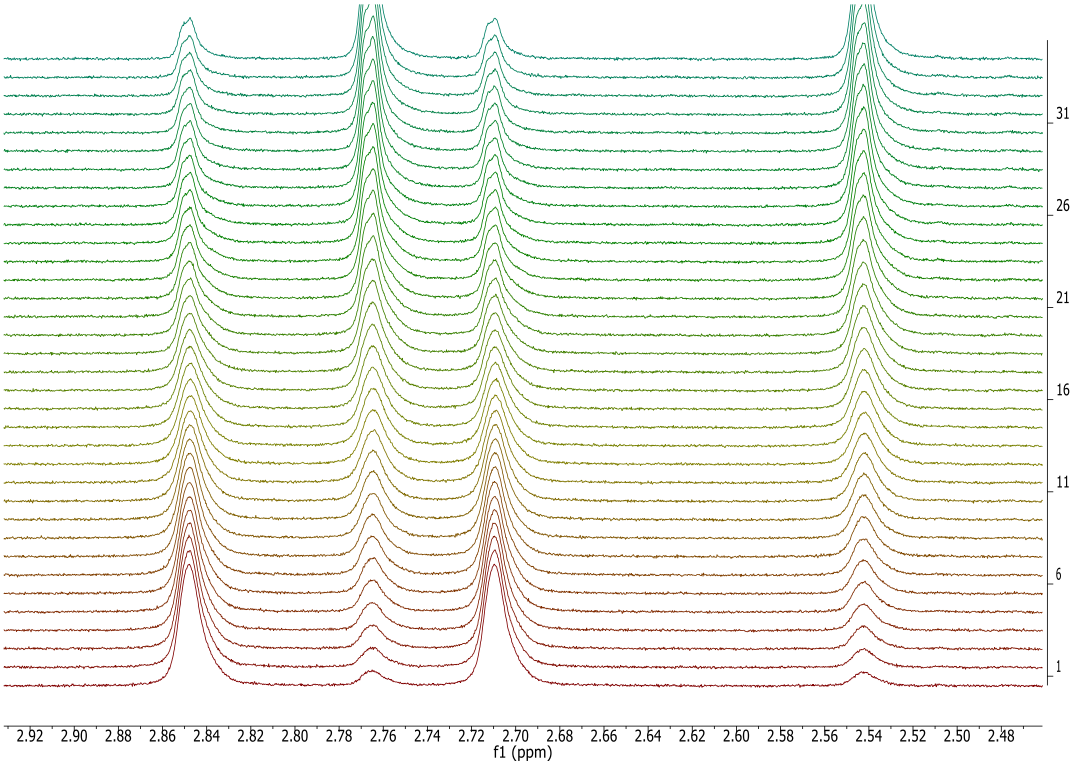

Figure S20. Isomerization of complex **4** to complex **4-THF** tracked via ^{1}H NMR over time with spectra taken 5 minutes apart; the bottom spectrum was taken at t = 15 min. Only the methylene protons for **4** (2.71 and 2.85 ppm) and **4-THF** (2.54 and 2.77 ppm) are shown. (Initial concentration of **1** = 1.857 x 10^{-2} M; 25 °C)

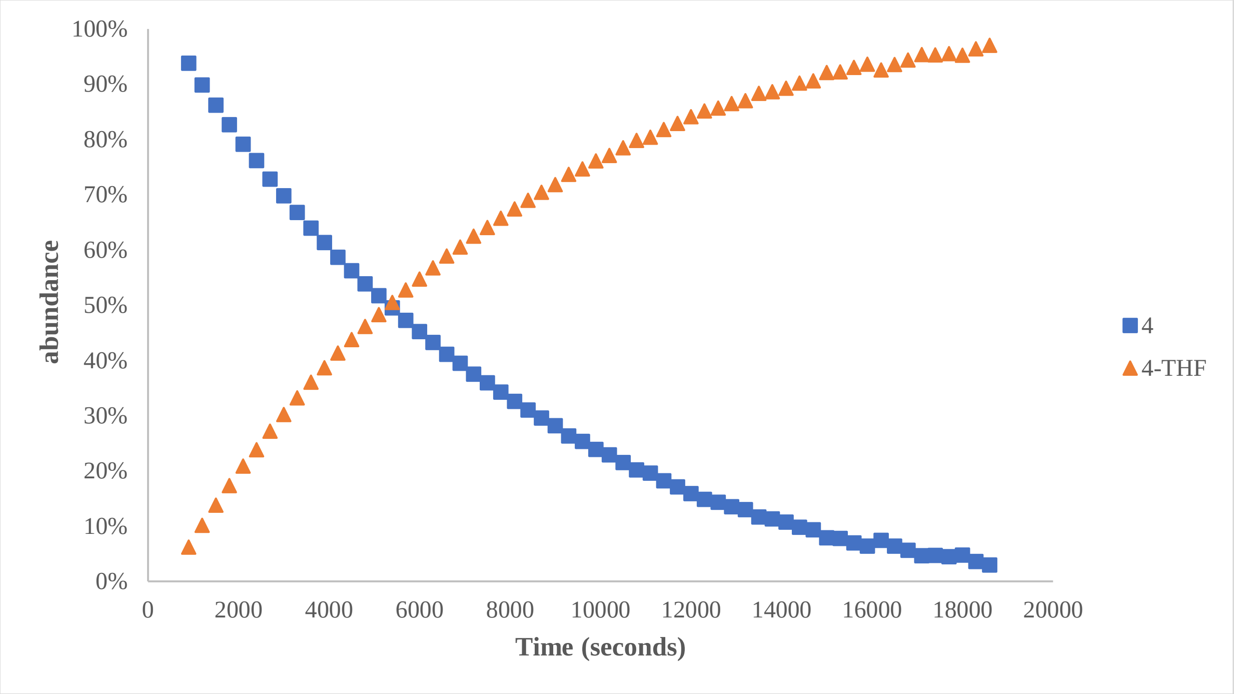

Figure S21. Conversion of the **4** into an equilibrium mixture of **4**/**4-THF**. This process has a half-life of 89.0 min. (Initial concentration of **1** = 1.857 x 10^{-2} M; 25 °C)

Table S5. % Abundance versus Time for the conversion of **4** to **4-THF**.

Time (sec)	4	4-THF
900	94	6
1200	90	10
1500	86	14
1800	83	17
2100	79	21
2400	76	24
2700	73	27
3000	70	30
3300	67	33
3600	64	36
3900	61	39
4200	59	41
4500	56	44
4800	54	46
5100	52	48
5400	49	51
5700	47	53
6000	45	55
6300	43	57
6600	41	59
6900	39	61

7200	38	62
7500	36	64
7800	34	66
8100	33	67
8400	31	69
8700	30	70
9000	28	72
9300	26	74
9600	25	75
9900	24	76
10200	23	77
10500	22	78
10800	20	80
11100	20	80
11400	18	82
11700	17	83
12000	16	84
12300	15	85
12600	14	86
12900	14	86
13200	13	87
13500	12	88
13800	11	89
14100	11	89
14400	10	90
14700	9	91
15000	8	92
15300	8	92
15600	7	93
15900	6	94
16200	7	93
16500	6	94
16800	6	94
17100	5	95
17400	5	95
17700	4	96
18000	5	95
18300	4	96
18600	3	97

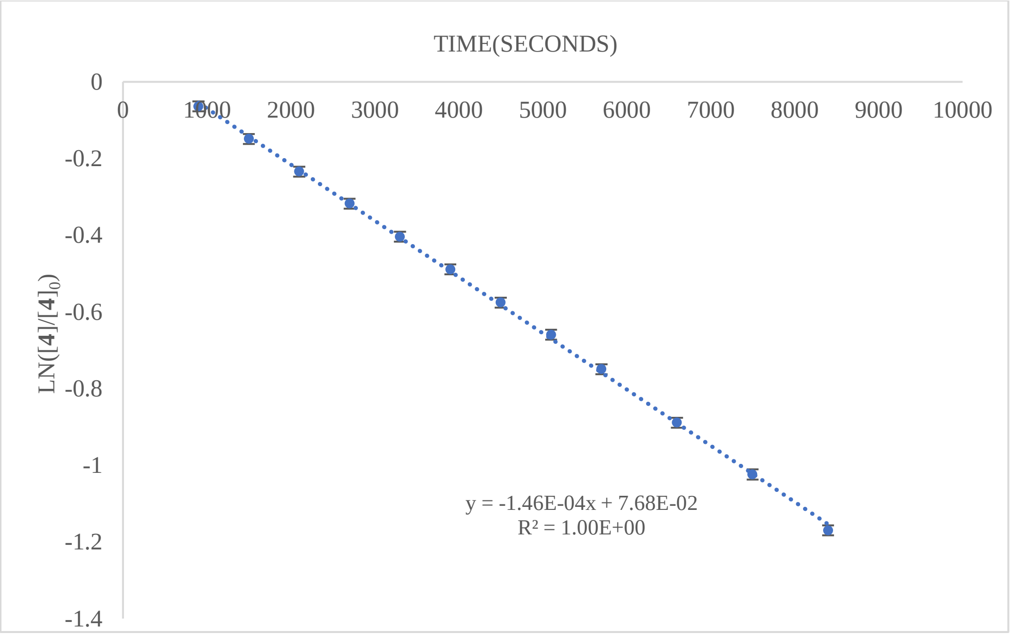

Figure S22. $\boldsymbol{ln}\frac{[\mathbf{4}]}{[\mathbf{4}]_0}$ vs. time graph for the conversion from **4** to **4-THF**, trial one. (Initial concentration of **1** = 1.857 x 10^{-2} M; 25 °C)

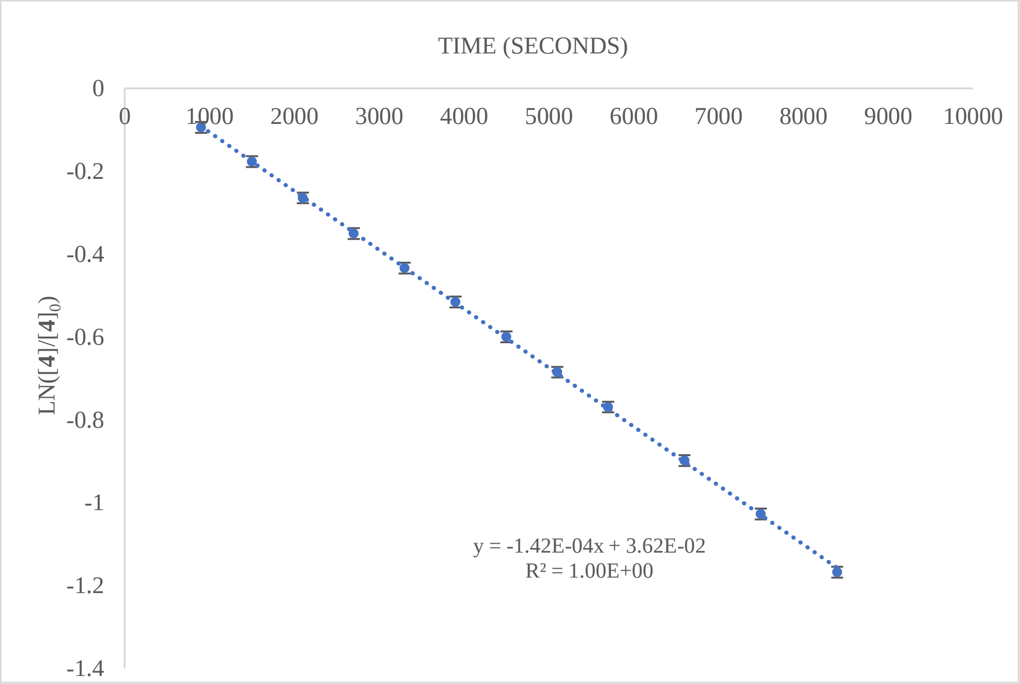

Figure S23. $\boldsymbol{ln}\frac{[\mathbf{4}]}{[\mathbf{4}]_0}$ vs. time graph for the conversion from **4** to **4-THF**, trial two. (Initial concentration of **1** = 1.857 x 10^{-2} M; 25 °C)

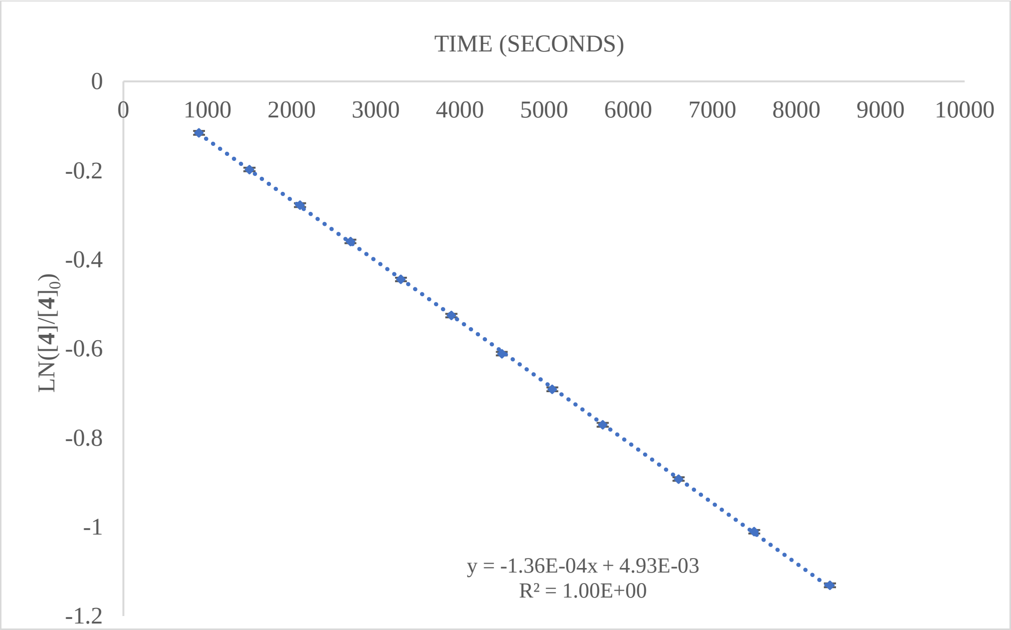

Figure S24. $\boldsymbol{ln}\frac{[\mathbf{4}]}{[\mathbf{4}]_\mathbf{0}}$ vs. time graph for the conversion from **4** to **4-THF**, trial three. (Initial concentration of **1** = 1.857 x 10^{-2} M; 25 °C)

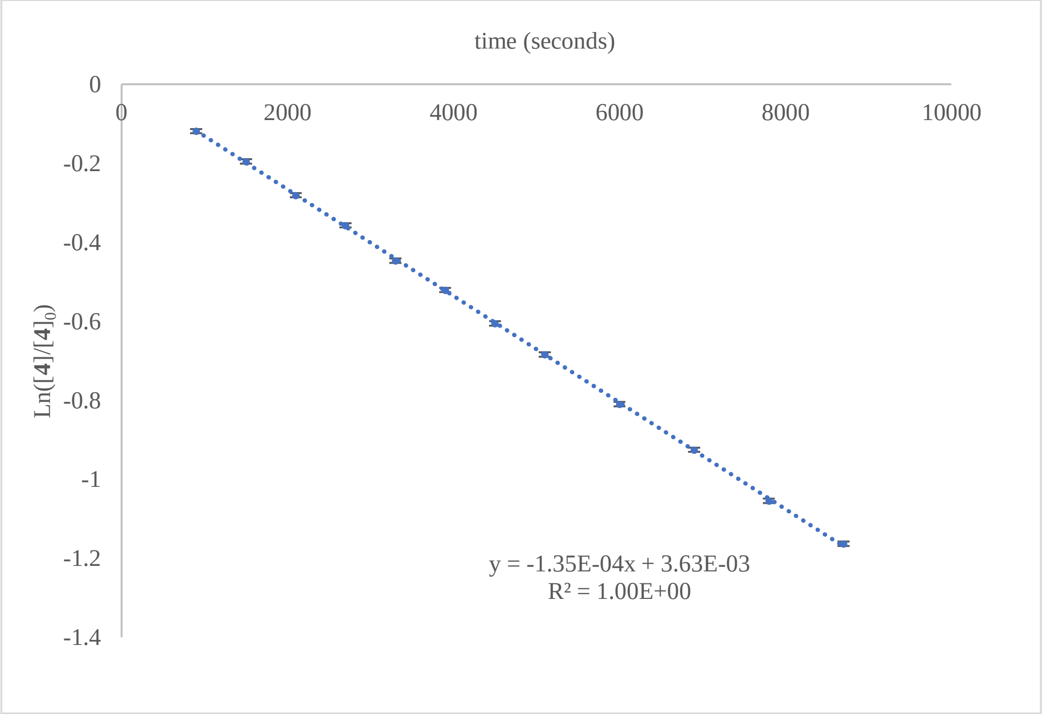

Figure S25. $\boldsymbol{ln}\frac{[\mathbf{4}]}{[\mathbf{4}]_\mathbf{0}}$ vs. time graph for the conversion from **4** to **4-THF** in the presence of a 10-fold excess of THF, trial one. (Initial concentration of **1** = 1.857 x 10^{-2} M; [THF] = 1.875 x 10^{-1} M, 25 °C)

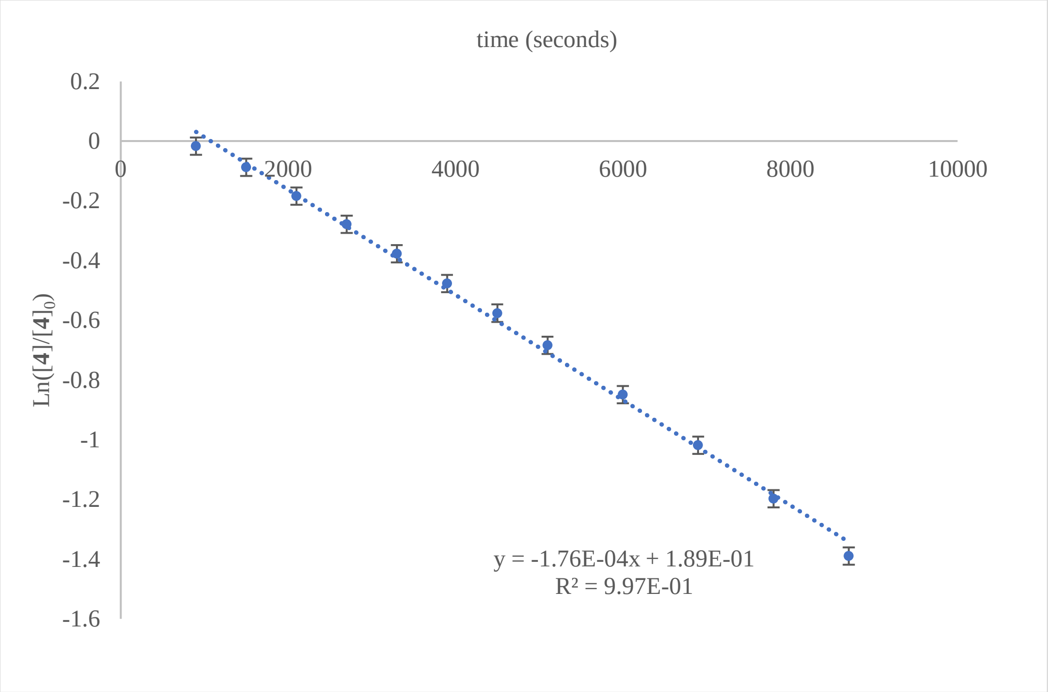

Figure S26. $\boldsymbol{ln}\frac{[\mathbf{4}]}{[\mathbf{4}]_0}$ vs. time graph for the conversion from **4** to **4-THF** in the presence of a 10-fold excess of THF, trial two. (Initial concentration of **1** = 1.857 x 10^{-2} M; [THF] = 1.875 x 10^{-1} M, 25 °C)

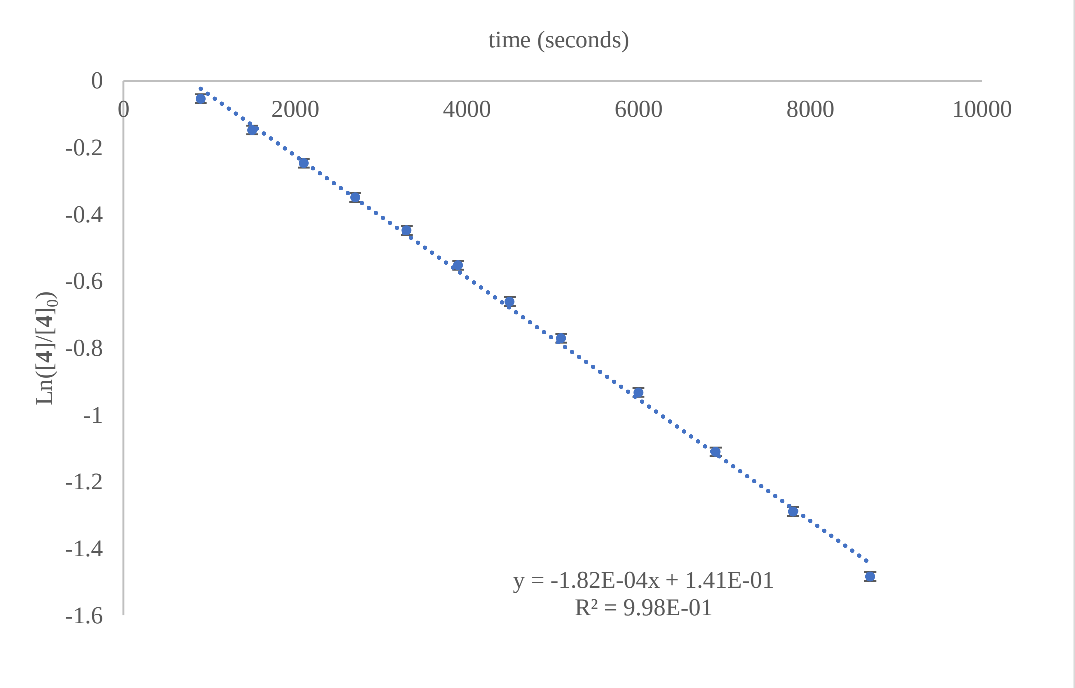

Figure S27. $\boldsymbol{ln}\frac{[\mathbf{4}]}{[\mathbf{4}]_0}$ vs. time graph for the conversion from **4** to **4-THF** in the presence of a 10-fold excess of THF, trial three. (Initial concentration of **1** = 1.857 x 10^{-2} M; [THF] = 1.875 x 10^{-1} M, 25 °C)

General Polymerization Procedures

In an inert atmosphere glove box, a 20 mL vial was charged with 2 mL of toluene. Phenylacetylene (300 µL, 279 mg, 2.73 mmol) was added via micropipette. The catalyst **4** (546 nmol) was added via micropipette from a stock solution (5 mg/mL) in one shot to initiate polymerization. This solution was allowed to stir for 20 min and then quenched by removing the vial from the glove box and pouring into excess methanol. The resulting polymers were isolated via filtration and residual solvent removed in vacuo. Note: catalyst **4** was generated *in situ* by adding dipropargylfluroene to complex **3** dissolved in 2 mL of toluene. This solution was allowed to stir for 5 min prior to addition of phenylacetylene to initiate polymerization.

Polymerization Kinetic Data

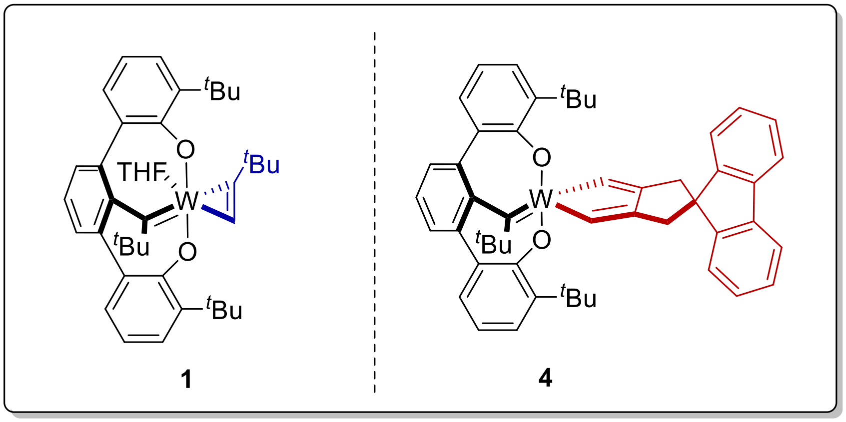

Table S6. Yield and activity for catalysts **1** and **4.**

	% Yield		**Activity (g_{pol}/mol_{cat}/h)**		**Isolated yield (mg)**	
Time (min)	**1**	**4**	**1**	**4**	**1**	**4**
5	20	12	1.28×10^6	0.73×10^6	56	32
10	42	17	1.34×10^6	0.52×10^6	118	46
15	58	30	1.24×10^6	0.63×10^6	163	83
20	56	26	0.88×10^6	0.42×10^6	155	73
25	66	38	0.84×10^6	0.48×10^6	184	106

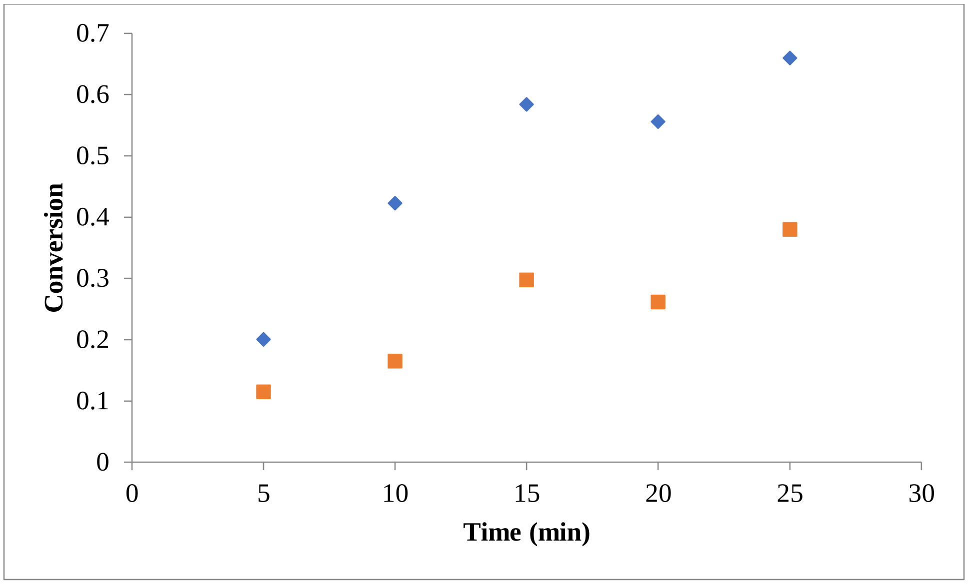

Figure S28. Conversion comparison with respect to time for the previously published catalyst **1** (blue) and the new dipropargylfluorene catalyst **4** (orange).

GPC Data

Table S7. Molecular weight and dispersity data

Sample	M_n (g/mol) x 10^4	M_w/M_n
1-5 min	15.7	2.00
1-10 min	18.4	1.81
1-15 min	9.4	1.94
1-20 min	11.6	2.28
1-25 min	11.2	1.90
4-5 min	6.9	2.04
4-10 min	6.6	1.88
4-15 min	8.8	1.83
4-20 min	7.8	1.89
4-25 min	6.0	1.90

Computational Methods

All ground state density functional theory (DFT) calculations were performed using the Gaussian 09 program.[6] The atomic coordinates of the modeled complexes **4'** and **(4-THF)'** were obtained from X-ray crystal structures and further edited using the program *ArgusLab*. Geometry optimization calculations on the W-alkylidyne complexes, **4'** and **(4-THF)'** described herein either employed B3LYP[7],[8] or the M06[9] functionals. For the elements C, H, and O, the triple zeta 6-311G(d,p)[10,11,12] basis set was used while the LANL2DZ[13,14,15] basis set with effective core potentials (ECP) was used for the W-atom. All calculations included a solvent sphere described by the SMD model,[16] with benzene as the solvent. Frequency analysis was performed using the same level of theory as the optimization to confirm absence of imaginary frequencies. Single point analysis were carried out using the following basis set combinations: (a) 6-311G(d,p) on the lighter atoms in conjunction with LANL2DZ (with ECP) for W, or (b) the Def2TZVP[17,18] basis set on all atoms (with ECP for W), or (c) the Def2TZVP basis set (with ECP) for W in conjunction with 6-311G(d,p) for the lighter atoms. Molecular orbital images were obtained using the program *Gabedit*,[19] with isovalue of 0.05 (number of points used during orbital image generation: 200).

Computed model complexes 4' and (4-THF)'

In the model complexes **4'** and **(4-THF)'**, the *ortho* tert-butyl groups on the pincer ligands were replaced with methyl groups to expedite the calculations. The structural parameters of the model complexes **4'** and **(4-THF)'** were compared to (a) the metric parameters of the tetraanionic W-metallacyclopentadiene complex, $[O_2C(^tBuC=)]W(\kappa^2\text{-}C(Ph)=C(H)C(Ph)=C(Me))$,[1] and (b) Pyykkö's Single-, Double-, and Triple bond Covalent radii.[20]

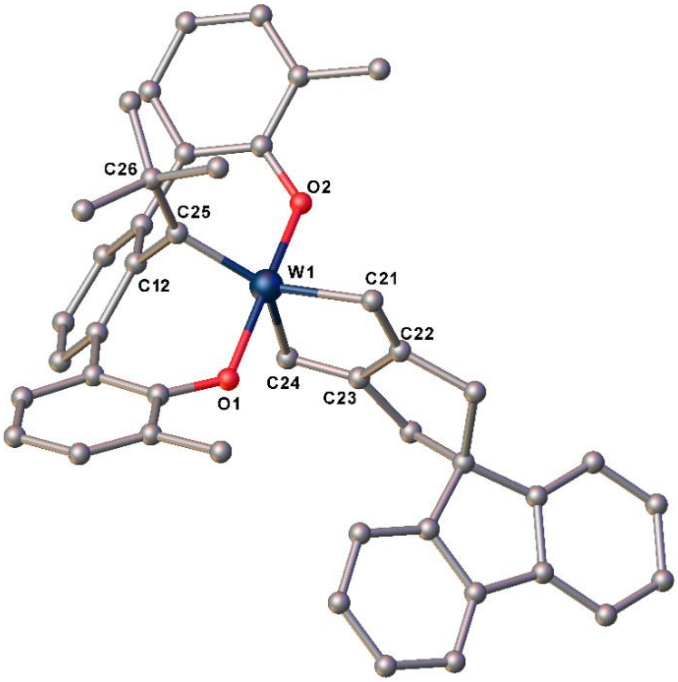

Figure S29. DFT computed structure of complex 4 using M06/ 6-311G(d,p)/ LANL2DZ level of theory. Complex **4'** also modeled with B3LYP/ 6-311G(d,p)/ LANL2DZ level of theory resembles the structure presented in **Figure S28** with some minor differences discussed below.

Table S8. Comparison of the structural parameters of model complex **4'**

	B3LYP^{a}	M06^{a}	[O$_2$C(^{t}BuC=)]W(mcp)^{b}
d W1=C25 (Å)	1.897	1.879	1.884(4)
d C12—C25 (Å)	1.489	1.479	1.500(5)
d C25—C26 (Å)	1.520	1.503	1.526(5)
d W1—O1 (Å)	2.013	2.008	1.972(2)
d W1—O2 (Å)	2.015	2.004	1.976(2)
d W1—C21 (Å)	2.071	2.066	2.062(4)
d W1—C24 (Å)	2.075	2.061	2.070(4)
d C21=C22 (Å)	1.358	1.352	1.354(6)
d C23=C24 (Å)	1.350	1.343	1.342(5)
d C22—C23 (Å)	1.498	1.500	1.495(5)
∠C12—C25—W1 (°)	94.26	93.76	92.4(3)
∠O1—W1—O2 (°)	169.34	169.91	166.74(11)
∠C25—W1—C21 (°)	138.33	137.33	133.91(17)
∠C25—W1—C24 (°)	129.28	128.51	131.03(16)
∠C21—W1—C24 (°)	92.38	94.13	95.06(16)

a – basis sets used: 6-311G(d,p) for C, H, O; LANL2DZ with ECP for W; benzene as solvent using the SMD model
b - [O$_2$C(^{t}BuC=)]W(κ^2-C(Ph)=C(H)C(Ph)=C(Me)); mcp = metallacyclopentadiene
Sum of covalent radii (Pyykkö): W=C 1.87 Å; W—O 2.00 Å; W—C 2.04 to 2.12 Å; C=C 1.34 Å; C—C 1.50 Å

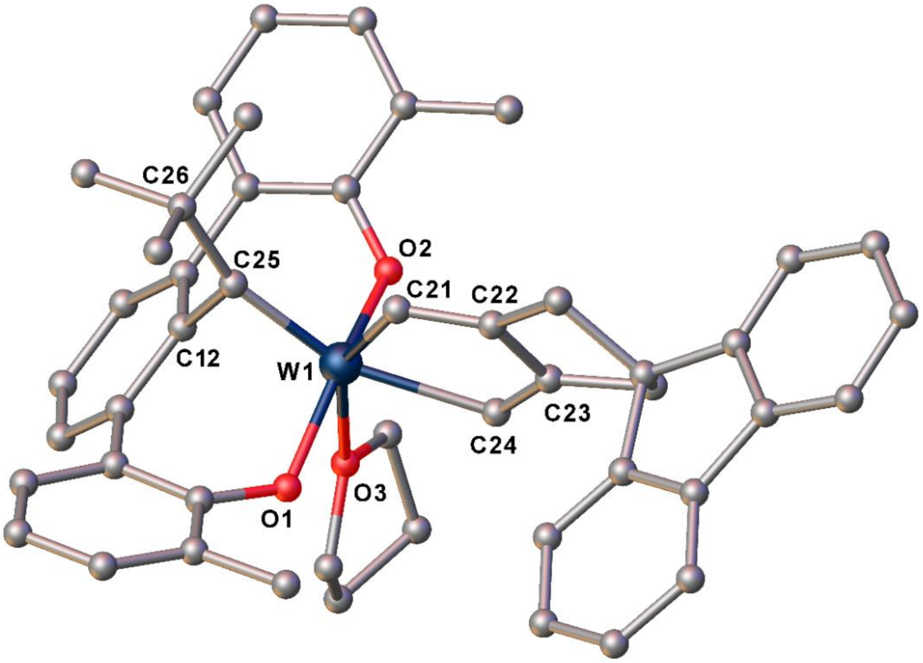

Figure S30. DFT computed structure of complex **(4-THF)'** using M06/ 6-311G(d,p)/ LANL2DZ level of theory. Complex **(4-THF)'** also modeled with B3LYP/ 6-311G(d,p)/ LANL2DZ level of theory resembles the structure presented in **Figure S29** with some minor differences discussed below.

Table S9. Comparison of structural parameters of model complex **(4-THF)'**

	B3LYP[a]	M06[a]	[O$_2$C(^{t}BuC=)]W(mcp)[b]
d W1=C25 (Å)	1.915	1.898	1.884(4)
d C12—C25 (Å)	1.539	1.536	1.500(5)
d C25—C26 (Å)	1.534	1.514	1.526(5)
d W1—O1 (Å)	1.965	1.972	1.972(2)
d W1—O2 (Å)	1.985	1.975	1.976(2)
d W1—O3 (Å)	2.405[c]	2.335[c]	N/A
d W1—C21 (Å)	2.160	2.142	2.062(4)
d W1—C24 (Å)	2.226	2.228	2.070(4)
d C21=C22 (Å)	1.346	1.345	1.354(6)
d C23=C24 (Å)	1.333	1.330	1.342(5)
d C22—C23 (Å)	1.473	1.468	1.495(5)
∠C12—C25—W1 (°)	87.82	85.60	92.4(3)
∠O1—W1—O2 (°)	152.57	156.53	166.74(11)
∠C25—W1—C21 (°)	80.89	81.59	133.91(17)
∠C25—W1—C24 (°)	151.53	154.65	131.03(16)
∠C21—W1—C24 (°)	74.05	74.67	95.06(16)

a – basis sets used: 6-311G(d,p) for C, H, O; LANL2DZ with ECP for W; benzene as solvent using the SMD model

b - [O$_2$C(^{t}BuC=)]W(κ^2-C(Ph)=C(H)C(Ph)=C(Me)) is 5-coordinate and has NO bound THF;

Sum of covalent radii (Pyykkö): W=C 1.87 Å; W—O 2.00 Å; W—C 2.04 to 2.12 Å; C=C 1.34 Å; C—C 1.50 Å

c – The W—THF distance is 2.288(3) Å in [O$_2$C(PhC=)W(η^2-MeC≡C^{t}Bu)(THF)],[1] 2.323(2) Å in [O$_2$C(PhC=)W(η^2-HC≡C^{t}Bu)(THF)],[1] 2.328(1) Å in [O$_2$C(^{t}BuC=)W(η^2-HC≡C^{t}Bu)(THF)],[2] and 2.473(2) Å for the THF disposed *anti* to the W-alkylidyne in [OCO]W≡C^{t}Bu(THF)$_2$.[3]

Thermochemistry for the conversion of 4' to (4-THF)'

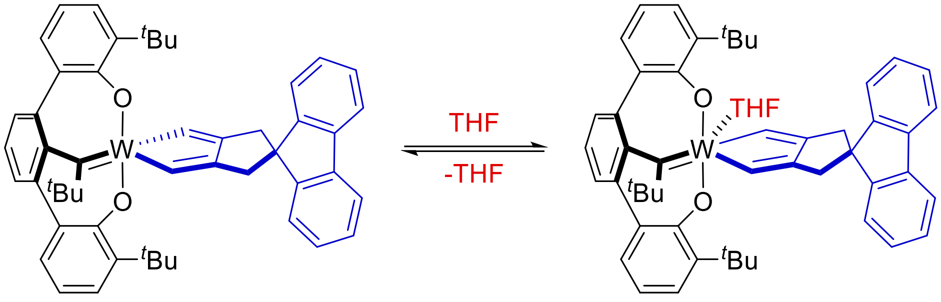

4' **(4-THF)'**

The data presented in **Table S10** is obtained from Frequency calculations for each of **4'**, **(4-THF)'**, and **THF** using the M06 functional and a combination of 6-311G(d,p) and LANL2DZ as the basis sets. For **THF**, 6-311G(d,p) was used as the basis set. All calculations were carried out with a benzene solvent sphere using the SMD model.

Table S10. Calculated thermochemistry values (in Hartrees) from Gaussian for the conversion of **4'** to **(4-THF)'** using M06 functional.

M06/ 6-311G(d,p)/ LANL2DZ level of theory

	4'	**THF**	**(4-THF)'**
ε_o	−1916.894423	−232.350104	−2149.270666
ε_{ZPE}	0.685265	0.115902	0.803304
E_{tot}	0.725166	0.120801	0.849503
H_{corr}	0.726110	0.121745	0.850447
G_{corr}	0.616292	0.087688	0.726570
$\varepsilon_o + \varepsilon_{ZPE}$	−1916.209158	−232.234202	−2148.467362
$\varepsilon_o + E_{tot}$	−1916.169258	−232.229304	−2148.421163
$\varepsilon_o + H_{corr}$	−1916.168314	−232.228359	−2148.420218
$\varepsilon_o + G_{corr}$	−1916.278132	−232.262416	−2148.544096

Enthalpy of the reaction:

$$\Delta_r \mathrm{H}° \text{ (298K)} = \Sigma(\,\varepsilon_o + H_{corr})_{\text{products}} - \Sigma(\,\varepsilon_o + H_{corr})_{\text{reactants}}$$

$$= [(-2148.420218) - ((-1916.168314) + (-232.228359))] \text{ x } 627.5095$$

$$= -0.023545 \text{ x } 627.5095$$

$$\Delta_r \mathrm{H}° \text{ (298K)} = -14.77 \text{ kcal/ mol}$$

Gibbs free energy of the reaction:

$$\Delta_r \mathrm{G}° \text{ (298K)} = \Sigma(\,\varepsilon_o + G_{corr})_{\text{products}} - \Sigma(\,\varepsilon_o + G_{corr})_{\text{reactants}}$$

$$= [(-2148.544096) - ((-1916.278132) + (-232.262416))] \text{ x } 627.5095$$

$$= -0.003548 \text{ x } 627.5095$$

$$\Delta_r \mathrm{G}° \text{ (298K)} = -2.23 \text{ kcal/ mol}$$

Frontier Molecular Orbitals of 4' and Comparison of orbital energies

Single point analysis of **4'** were carried out using the following basis set combinations with M06 as the functional. (a) 6-311G(d,p) on the lighter atoms in conjunction with LANL2DZ (with ECP) for W, or (b) the Def2TZVP basis set on all atoms (with ECP for W), or (c) the Def2TZVP basis set (with ECP) for W in conjunction with 6-311G(d,p) for the lighter atoms. Molecular orbital images were obtained using the program *Gabedit*, with isovalue of 0.05 (number of points used during orbital image generation: 200). All calculations included a solvent sphere described by the SMD model, with benzene as the solvent.

Table S11. Comparison of frontier molecular orbital energies of **4'** using different levels of theory

Frontier Orbital energies (eV)	M06		
	6-311G(d,p) and LANL2DZ	6-311G(d,p) and Def2TZVP	Def2TZVP
HOMO	−5.742	−5.740	−5.723
LUMO	−2.109	−1.995	−1.995
HOMO(-2)	−6.172	−6.142	−6.123
HOMO(-6)	−6.844	−6.853	−6.851
LUMO(+1)	−1.562	−1.545	−1.558

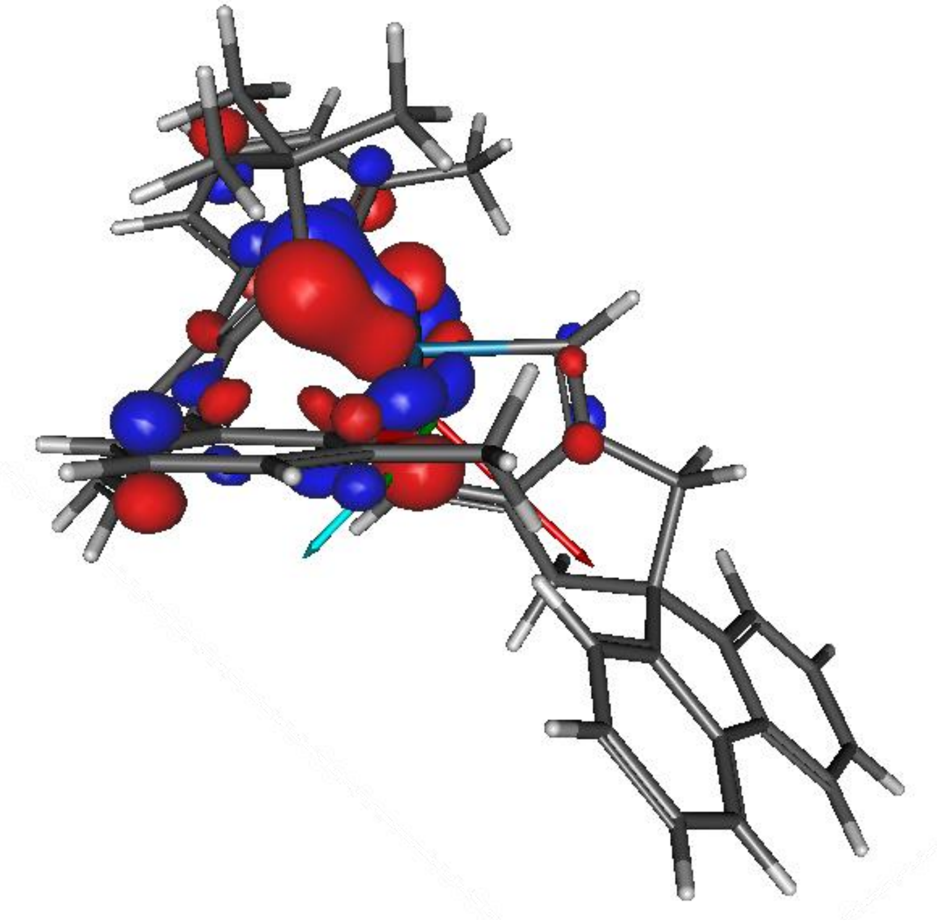

Figure S31. HOMO [−5.742 eV] of the geometry optimized structure of **4'** (isovalue - 0.05)

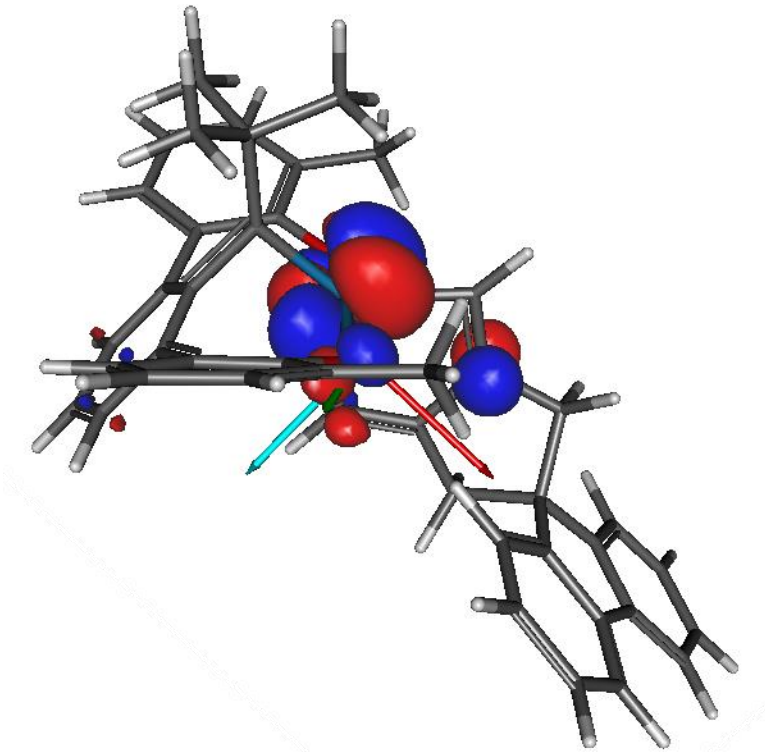

Figure S32. LUMO [−2.109 eV] of the geometry optimized structure of **4'** (isovalue - 0.05)

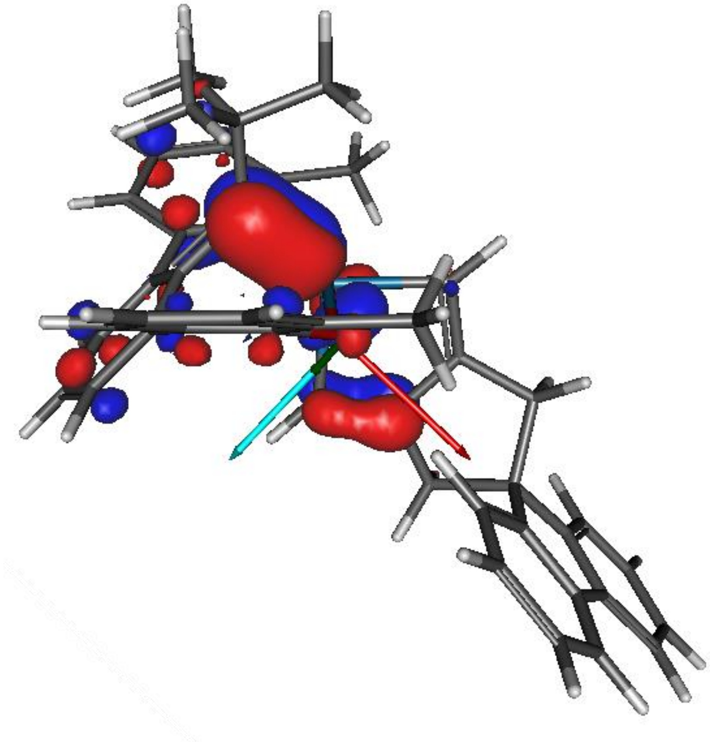

Figure S33. HOMO(−2) [−6.172 eV] of the geometry optimized structure of **4'** (isovalue - 0.05)

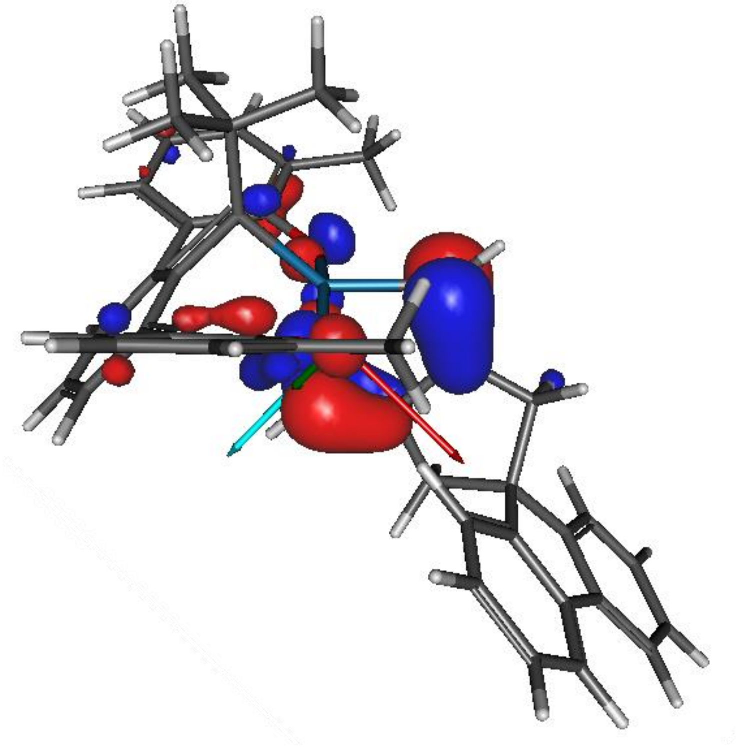

Figure S34. HOMO(−6) [−6.844 eV] of the geometry optimized structure of **4'** (isovalue - 0.05)

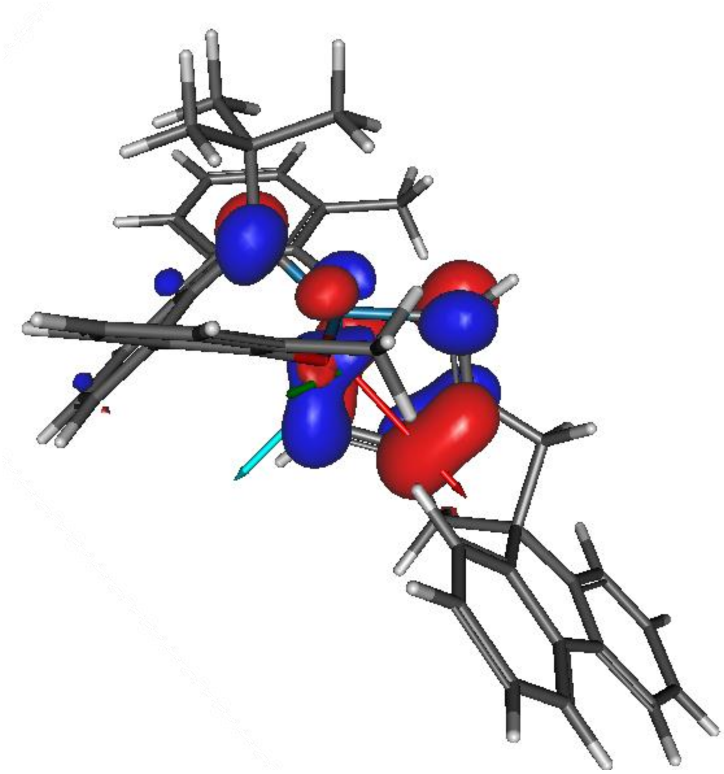

Figure S35. LUMO(+1) [−1.562 eV] of the geometry optimized structure of **4'** (isovalue - 0.05)

Frontier Molecular Orbitals of (4-THF)' and Comparison of orbital energies

Single point analysis of (**4-THF)'** were carried out using the following basis set combinations with M06 as the functional. (a) 6-311G(d,p) on the lighter atoms in conjunction with LANL2DZ (with ECP) for W, or (b) the Def2TZVP basis set on all atoms (with ECP for W), or (c) the Def2TZVP basis set (with ECP) for W in conjunction with 6-311G(d,p) for the lighter atoms. Molecular orbital images were obtained using the program *Gabedit*, with isovalue of 0.05 (number of points used during orbital image generation: 200). All calculations included a solvent sphere described by the SMD model, with benzene as the solvent.

Table S12. Comparison of frontier molecular orbital energies of (**4-THF)'** using different levels of theory

Frontier Orbital energies (eV)	M06		
	6-311G(d,p) and LANL2DZ	6-311G(d,p) and Def2TZVP	Def2TZVP
HOMO	−5.461	−5.449	−5.451
LUMO	−2.107	−2.010	−2.005
HOMO(−3)	−6.351	−6.311	−6.301

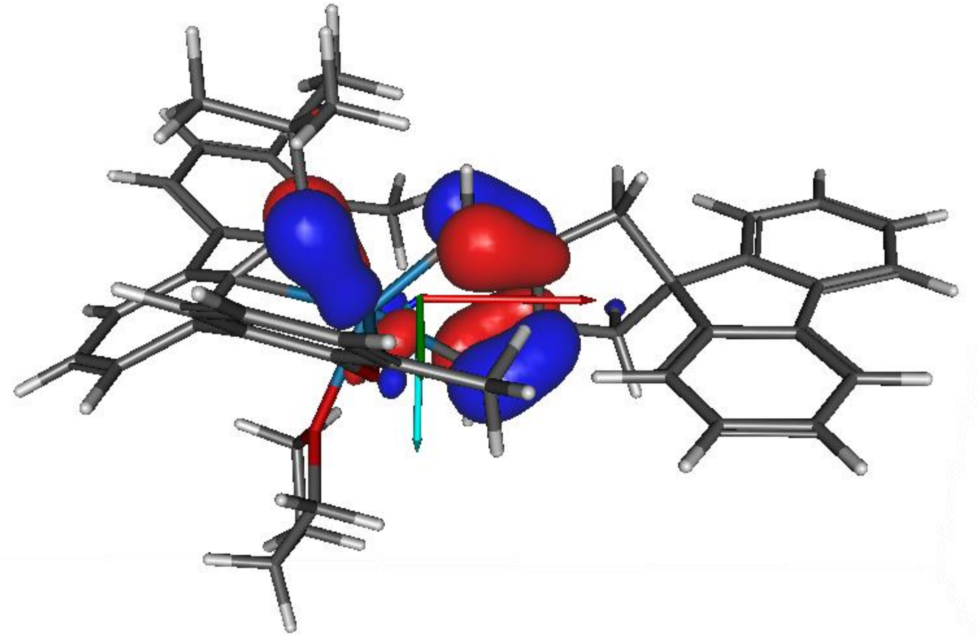

Figure S36. HOMO [−5.461 eV] of the geometry optimized structure of **(4-THF)'** (isovalue – 0.05)

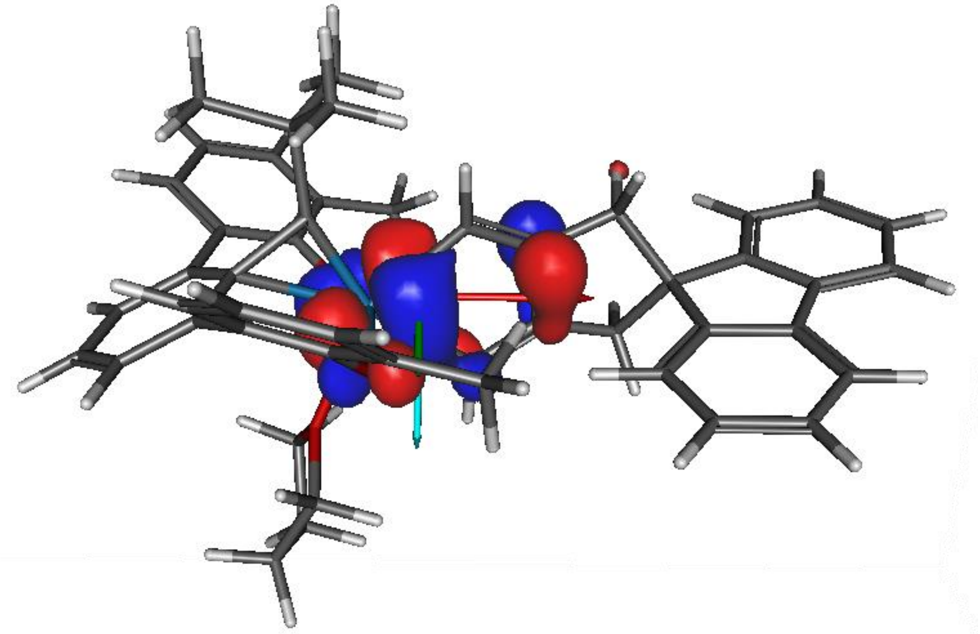

Figure S37. LUMO [−2.107 eV] of the geometry optimized structure of **(4-THF)'** (isovalue – 0.05)

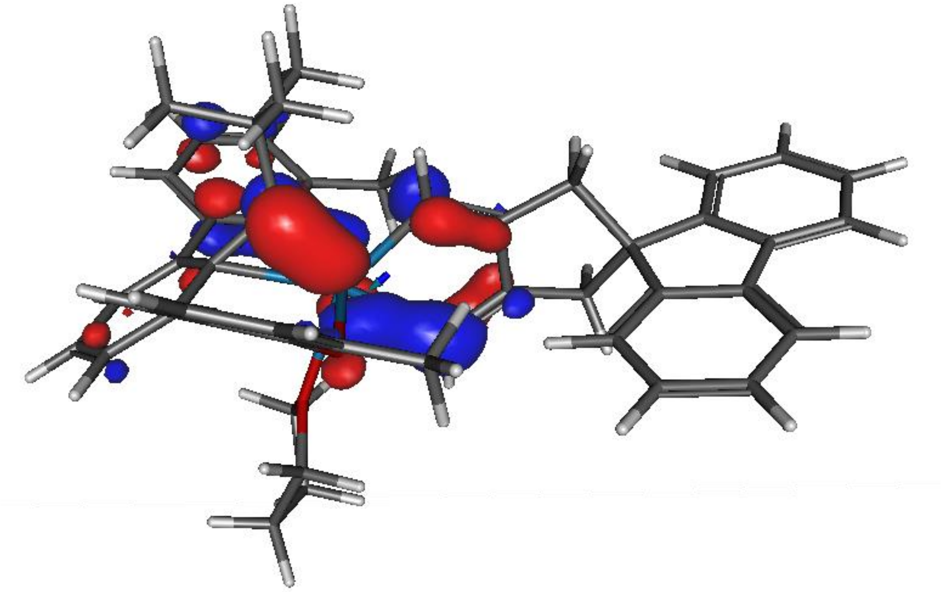

Figure S38. HOMO(−3) [−6.351 eV] of the geometry optimized structure of **(4-THF)'** (isovalue – 0.05)

Atomic coordinates of 4' and (4-THF)'

Table S13. Atomic coordinates of geometry optimized structure of **4'** using B3LYP functional and (6-311G(d,p)/ LANL2DZ) basis sets in a benzene solvent sphere using the SMD solvent model

	X	Y	Z
W	-0.86451	-0.11296	-0.50228
O	-0.5147	1.86216	-0.33732
O	-1.14104	-2.09833	-0.30056
C	-1.32289	2.87143	0.00804
C	-1.03555	4.14187	-0.54875
C	-1.82037	5.2343	-0.19462
C	-2.87654	5.10399	0.70747
C	-3.1475	3.86246	1.2609
C	-2.39668	2.7222	0.92564
C	-2.72342	1.43908	1.61431
C	-2.88271	1.44316	3.00551
C	-3.17112	0.26896	3.69258
C	-3.2746	-0.94075	3.0146
C	-3.12198	-0.99839	1.62379
C	-2.89731	0.21355	0.91159
C	-3.20439	-2.32685	0.94998
C	-4.27263	-3.17756	1.28325
C	-4.38374	-4.45249	0.75053
C	-3.39761	-4.91847	-0.12002
C	-2.31093	-4.12405	-0.46922
C	-2.21488	-2.81107	0.05385
C	0.10841	4.27863	-1.518
C	-1.22934	-4.62711	-1.38843
C	0.7062	-0.38628	-1.82352
C	1.72285	-0.57656	-0.94351
C	1.56073	-0.54317	0.5451
C	0.37717	-0.30691	1.14918
C	-2.73706	0.1847	-0.56892
C	-3.79731	0.33301	-1.64752
C	-4.53606	1.68315	-1.51078
C	-4.84227	-0.80127	-1.55322
C	-3.11535	0.26971	-3.03003
C	2.9061	-0.84176	1.17928
C	3.96348	-0.57015	0.06475
C	3.17614	-0.87761	-1.24857
C	4.51092	0.85659	0.10044
C	3.82646	2.06568	0.05415
C	4.55256	3.25965	0.10276

C	5.94522	3.24448	0.19603
C	6.63725	2.03537	0.24869
C	5.91508	0.84335	0.20567
C	6.36827	-0.55198	0.26502
C	7.64934	-1.09342	0.37356
C	7.79334	-2.47928	0.41985
C	6.67403	-3.3122	0.35833
C	5.39084	-2.77018	0.24603
C	5.24103	-1.38985	0.19894
H	-1.60008	6.20301	-0.63244
H	-3.48226	5.96328	0.97167
H	-3.97439	3.75542	1.95399
H	-2.74586	2.36833	3.5526
H	-3.27663	0.29032	4.7719
H	-3.43912	-1.8571	3.56888
H	-5.0381	-2.81064	1.95791
H	-5.22842	-5.08048	1.00976
H	-3.47107	-5.91954	-0.53366
H	-3.85729	2.5291	-1.62498
H	-5.02963	1.77124	-0.54021
H	-5.3069	1.75609	-2.28541
H	-4.38712	-1.78327	-1.68871
H	-5.59883	-0.66532	-2.33361
H	-5.35344	-0.79419	-0.58833
H	-2.59379	-0.68175	-3.17632
H	-2.3964	1.08404	-3.16187
H	-3.85986	0.35852	-3.82706
H	0.86215	-0.40911	-2.8977
H	0.23862	-0.27042	2.22351
H	2.93867	-1.89995	1.46157
H	3.09049	-0.25715	2.08179
H	3.55243	-0.31791	-2.10622
H	3.27054	-1.94287	-1.48799
H	2.74512	2.0946	-0.01249
H	4.02709	4.20765	0.07133
H	6.49193	4.18042	0.23186
H	7.71902	2.02712	0.32739
H	8.52199	-0.45119	0.42317
H	8.7826	-2.91526	0.50474
H	6.80156	-4.38828	0.3971
H	4.52942	-3.42871	0.19659
H	0.20471	5.31092	-1.86146
H	-0.02968	3.63809	-2.39456

H	1.05638	3.97748	-1.06338
H	-1.43596	-5.65095	-1.70772
H	-0.2521	-4.60923	-0.89658
H	-1.1352	-4.00181	-2.28164

Table S14. Atomic coordinates of geometry optimized structure of **4'** using M06 functional and (6-311G(d,p)/ LANL2DZ) basis sets in a benzene solvent sphere using the SMD solvent model

	X	Y	Z
W	-0.82893	-0.23404	-0.46016
O	-0.17209	1.6605	-0.35246
O	-1.39564	-2.14205	-0.22718
C	-0.85665	2.76891	-0.08675
C	-0.49656	3.93324	-0.79277
C	-1.15693	5.12062	-0.51842
C	-2.15475	5.18689	0.4474
C	-2.50597	4.04149	1.13606
C	-1.89026	2.81409	0.87378
C	-2.33291	1.62247	1.63548
C	-2.40249	1.67392	3.0257
C	-2.80474	0.56381	3.75325
C	-3.12805	-0.62373	3.11499
C	-3.07575	-0.72014	1.72574
C	-2.7184	0.42859	0.97937
C	-3.42178	-1.99963	1.06238
C	-4.62314	-2.62438	1.41044
C	-5.01888	-3.81037	0.82259
C	-4.19506	-4.40646	-0.1255
C	-2.98135	-3.84078	-0.48151
C	-2.58359	-2.62901	0.11617
C	0.5639	3.84339	-1.84251
C	-2.08572	-4.4684	-1.49958
C	0.64445	-0.69475	-1.8332
C	1.64598	-0.94068	-0.95917
C	1.51077	-0.91322	0.53478
C	0.38293	-0.56342	1.17426
C	-2.61722	0.34033	-0.4936
C	-3.63964	0.61797	-1.56001
C	-4.12103	2.06806	-1.48209
C	-4.84844	-0.30688	-1.39721
C	-2.98647	0.3666	-2.91934
C	2.85083	-1.27261	1.11807
C	3.85655	-0.87762	0.01752

C	3.08871	-1.2425	-1.26844
C	4.22542	0.59236	0.09653
C	3.40828	1.71203	0.06113
C	3.992	2.97045	0.18751
C	5.3671	3.10961	0.34267
C	6.18887	1.99126	0.37499
C	5.61149	0.73471	0.25302
C	6.2194	-0.59338	0.27
C	7.54559	-0.98763	0.38943
C	7.84394	-2.34373	0.37189
C	6.8338	-3.29125	0.23841
C	5.5048	-2.89626	0.12062
C	5.20356	-1.54654	0.13598
H	-0.8817	6.01252	-1.07746
H	-2.66039	6.12539	0.65152
H	-3.30257	4.0752	1.87555
H	-2.10644	2.58431	3.53949
H	-2.83638	0.61583	4.83766
H	-3.39606	-1.50004	3.6985
H	-5.2697	-2.13674	2.13614
H	-5.96622	-4.26619	1.09234
H	-4.49802	-5.33624	-0.6024
H	-3.3006	2.77746	-1.63331
H	-4.57749	2.28259	-0.5091
H	-4.87826	2.24734	-2.25611
H	-4.5686	-1.36163	-1.49159
H	-5.59366	-0.07757	-2.16975
H	-5.32382	-0.17046	-0.41914
H	-2.64753	-0.67549	-3.00923
H	-2.12411	1.03002	-3.07514
H	-3.69573	0.55339	-3.7346
H	0.7988	-0.70449	-2.90936
H	0.27175	-0.49907	2.25314
H	2.89947	-2.35953	1.28047
H	3.04891	-0.78188	2.07567
H	3.4516	-0.71142	-2.15378
H	3.19857	-2.32004	-1.46003
H	2.32815	1.63025	-0.05439
H	3.36069	3.85469	0.17233
H	5.79989	4.10074	0.44131
H	7.26358	2.09805	0.49809
H	8.33679	-0.24975	0.49277
H	8.87609	-2.66927	0.4621

H	7.08594	-4.34739	0.22651
H	4.72018	-3.643	0.01727
H	0.71252	4.81011	-2.33247
H	0.30145	3.10676	-2.61241
H	1.52563	3.51681	-1.42979
H	-2.52246	-5.39114	-1.89231
H	-1.10192	-4.70321	-1.07823
H	-1.90164	-3.78999	-2.34221

Table S15. Atomic coordinates of geometry optimized structure of **(4-THF)'** using B3LYP functional and (6-311G(d,p)/ LANL2DZ) basis sets in a benzene solvent sphere using the SMD solvent model

	X	Y	Z
W	-0.87338	-0.04092	0.23771
O	-0.89329	1.90977	0.46947
O	-1.39943	-1.88298	0.75936
C	-1.43811	2.86329	-0.31589
C	-0.68655	4.0284	-0.568
C	-1.25338	5.02791	-1.35613
C	-2.54174	4.90237	-1.87531
C	-3.28336	3.76379	-1.59509
C	-2.74841	2.72324	-0.81961
C	-3.58887	1.55498	-0.45859
C	-4.8781	1.79797	0.02751
C	-5.70316	0.74686	0.40881
C	-5.251	-0.56464	0.33253
C	-3.97013	-0.85763	-0.1511
C	-3.12707	0.21233	-0.58022
C	-3.55827	-2.28482	-0.22386
C	-4.46882	-3.24371	-0.70264
C	-4.14751	-4.59187	-0.73503
C	-2.90132	-5.01295	-0.26851
C	-1.97022	-4.10477	0.2269
C	-2.3014	-2.73142	0.24165
C	0.70179	4.16201	-0.00204
C	-0.62525	-4.54891	0.73743
C	0.77359	-0.11449	-1.15744
C	1.9753	-0.46401	-0.66148
C	2.07232	-0.7125	0.78758
C	0.93648	-0.49671	1.45154
C	-1.86529	-0.11449	-1.39876
C	-1.98928	-0.3933	-2.90174
C	-1.4355	0.8155	-3.70208

C	-3.45331	-0.58753	-3.3568
C	-1.21541	-1.67877	-3.27797
C	3.48655	-1.12045	1.12643
C	4.33975	-0.58802	-0.0798
C	3.33514	-0.65551	-1.28676
C	4.86116	0.82647	0.16373
C	4.15423	1.98554	0.46277
C	4.85555	3.17996	0.65385
C	6.24703	3.2149	0.5467
C	6.96256	2.05533	0.25046
C	6.2652	0.86282	0.06002
C	6.74606	-0.49069	-0.2433
C	8.03725	-0.9796	-0.44276
C	8.20967	-2.3357	-0.71706
C	7.10782	-3.19065	-0.79109
C	5.81398	-2.7005	-0.59376
C	5.63452	-1.34995	-0.32096
O	-1.71198	0.26476	2.4712
C	-1.97885	-0.82762	3.40516
C	-1.81753	-0.22	4.79341
C	-2.24567	1.23442	4.5659
C	-1.66069	1.53481	3.19148
H	-0.67269	5.92077	-1.56541
H	-2.96181	5.68876	-2.49183
H	-4.28585	3.65867	-1.9945
H	-5.22206	2.8202	0.13116
H	-6.69599	0.95318	0.79405
H	-5.88756	-1.37187	0.6743
H	-5.43119	-2.91264	-1.07613
H	-4.85761	-5.3119	-1.12534
H	-2.64484	-6.06748	-0.29158
H	-0.39764	1.04555	-3.46384
H	-2.02359	1.7148	-3.50837
H	-1.49294	0.59932	-4.77457
H	-3.91523	-1.45389	-2.88152
H	-3.47464	-0.75437	-4.4382
H	-4.06668	0.29163	-3.14564
H	-1.66404	-2.55247	-2.79984
H	-0.1687	-1.638	-2.97844
H	-1.25378	-1.83076	-4.36211
H	0.69987	0.1284	-2.20797
H	0.8609	-0.63858	2.53081
H	3.56079	-2.21411	1.156

H	3.84637	-0.74365	2.08564
H	3.57432	0.06614	-2.07033
H	3.38995	-1.65321	-1.73875
H	3.0746	1.96957	0.55461
H	4.31102	4.08851	0.88706
H	6.77545	4.15002	0.69749
H	8.04408	2.08521	0.17246
H	8.89662	-0.32011	-0.38611
H	9.20745	-2.7305	-0.87438
H	7.2573	-4.24324	-1.00505
H	4.96594	-3.37497	-0.65645
H	1.11103	5.15239	-0.21201
H	1.3761	3.41634	-0.4329
H	0.70938	4.00696	1.08039
H	-0.48884	-5.62209	0.58688
H	-0.51089	-4.33743	1.80511
H	0.18618	-4.02054	0.22969
H	-1.28744	-1.63673	3.18579
H	-2.99995	-1.17632	3.23047
H	-2.42478	-0.73947	5.53687
H	-0.77282	-0.26434	5.11426
H	-1.86945	1.92164	5.32587
H	-3.33658	1.31249	4.54168
H	-2.22492	2.26904	2.62151
H	-0.61757	1.85482	3.24771

Table S16. Atomic coordinates of geometry optimized structure of **(4-THF)'** using M06 functional and (6-311G(d,p)/ LANL2DZ) basis sets in a benzene solvent sphere using the SMD solvent model

	X	Y	Z
W	-0.84462	-0.07621	0.26306
O	-0.73608	1.88109	0.47498
O	-1.36696	-1.92309	0.7299
C	-1.29238	2.79798	-0.3278
C	-0.50243	3.86186	-0.78712
C	-1.09396	4.83076	-1.58563
C	-2.44083	4.77328	-1.92332
C	-3.21172	3.72062	-1.46473
C	-2.64902	2.71221	-0.67929
C	-3.47779	1.57914	-0.22921
C	-4.70062	1.82992	0.38764
C	-5.5121	0.78146	0.79097
C	-5.12014	-0.53271	0.59045

C	-3.90071	-0.82526	-0.01427
C	-3.06253	0.24014	-0.43939
C	-3.52705	-2.23661	-0.22828
C	-4.44902	-3.13282	-0.77747
C	-4.10854	-4.45312	-1.00594
C	-2.83104	-4.8976	-0.68017
C	-1.89387	-4.04868	-0.11162
C	-2.25572	-2.71403	0.12859
C	0.94816	3.90019	-0.43631
C	-0.50416	-4.48611	0.21801
C	0.76955	-0.29064	-1.12815
C	1.96041	-0.63981	-0.60969
C	2.06543	-0.81031	0.84499
C	0.95156	-0.51083	1.5072
C	-1.8579	-0.06617	-1.34136
C	-2.05236	-0.2463	-2.83229
C	-1.37777	0.92182	-3.56914
C	-3.52826	-0.23905	-3.23785
C	-1.45247	-1.58627	-3.27543
C	3.47349	-1.2068	1.18034
C	4.28968	-0.6664	-0.02449
C	3.31265	-0.86048	-1.21578
C	4.67646	0.78384	0.17628
C	3.86664	1.87843	0.4295
C	4.4569	3.1289	0.5923
C	5.83705	3.28092	0.50945
C	6.65413	2.18477	0.26506
C	6.06778	0.93719	0.09924
C	6.66499	-0.37417	-0.14651
C	7.9904	-0.76145	-0.29645
C	8.27367	-2.10228	-0.52199
C	7.24935	-3.0408	-0.59881
C	5.92158	-2.65252	-0.44788
C	5.63392	-1.31908	-0.22075
O	-1.74807	0.2279	2.39457
C	-2.12831	-0.85214	3.27828
C	-2.02388	-0.26666	4.66743
C	-2.40564	1.18493	4.42426
C	-1.69614	1.47495	3.12203
H	-0.47846	5.64976	-1.95121
H	-2.88144	5.542	-2.55025
H	-4.26063	3.64705	-1.74221
H	-5.00692	2.85718	0.5648

H	-6.45871	0.99127	1.28117
H	-5.75405	-1.34812	0.92777
H	-5.4338	-2.76675	-1.05876
H	-4.82744	-5.13346	-1.45117
H	-2.5499	-5.93011	-0.87618
H	-0.31382	1.01544	-3.33698
H	-1.85409	1.8735	-3.30579
H	-1.47659	0.78171	-4.65346
H	-4.0852	-1.05744	-2.76922
H	-3.60866	-0.36409	-4.32462
H	-4.01776	0.70638	-2.97582
H	-2.02074	-2.42267	-2.85152
H	-0.41183	-1.7018	-2.96042
H	-1.49125	-1.67269	-4.36914
H	0.71507	-0.11726	-2.19861
H	0.88992	-0.56886	2.60023
H	3.56288	-2.30345	1.2029
H	3.83969	-0.82493	2.13886
H	3.54011	-0.20934	-2.06636
H	3.39152	-1.8999	-1.56882
H	2.78797	1.76489	0.51337
H	3.83136	3.99517	0.78929
H	6.2791	4.26441	0.63968
H	7.73314	2.30321	0.20729
H	8.79269	-0.03034	-0.23926
H	9.30468	-2.42241	-0.64132
H	7.48998	-4.08483	-0.77664
H	5.12595	-3.39251	-0.50665
H	1.41845	4.81561	-0.80706
H	1.47854	3.04463	-0.87325
H	1.09805	3.84297	0.64775
H	-0.34574	-5.53376	-0.05309
H	-0.28285	-4.36673	1.28482
H	0.23188	-3.87134	-0.31607
H	-1.46826	-1.69985	3.08975
H	-3.15839	-1.14737	3.03147
H	-2.67003	-0.7812	5.38228
H	-0.99019	-0.33021	5.02948
H	-2.09569	1.8637	5.22209
H	-3.49097	1.27706	4.29343
H	-2.16852	2.24785	2.51208
H	-0.64296	1.74435	3.27391

References

---

[1] McGowan, K. P.; O'Reilly, M. E.; Ghiviriga, I.; Abboud, K. A.; Veige, A. S. Compelling mechanistic data and identification of the active species in tungsten-catalyzed alkyne polymerizations: conversion of a trianionic pincer into a new tetraanionic pincer-type ligand. *Chem. Sci*., **2013**, *4*, 1145−1155.

[2] Roland, C. D.; Li, H.; Abboud, K. A.; Wagener, K. B.; Veige, A. S. Cyclic polymers from alkynes. *Nat. Chem*. **2016**, *8*, 791−796

[3] Sarkar, S.; McGowan, K. P.; Kuppuswamy, S.; Ghiviriga, I.; Abboud, K. A.; Veige, A. S. An OCO^{3-} trianionic pincer tungsten(VI) alkylidyne: rational design of a highly active alkyne polymerization catalyst. *J. Am. Chem. Soc.* **2012**, *134*, 4509−4512.

[4] Mastrorilli, P.; Nobile, C. F.; Rizzuti, A.; Suranna, G. P.; Acierno, D.; Amendola, E. Polymerization of phenylacetylene and of p-tolylacetylene catalyzed by β-dioxygenato rhodium(I) complexes in homogeneous and heterogeneous phase. *J. Mol. Catal. A-Chem.* **2002**, *178*, 35−42

[5] Trhlíková, O.; Zedník, J.; Balcar, H.; Brus, J.; Sedláček, J. [Rh(cycloolefin)(acac)] complexes as catalysts of polymerization of aryl- and alkylacetylenes: Influence of cycloolefin ligand and reaction conditions. *J. Mol. Catal. A: Chem*. **2013**, *378*, 57−66

[6] Gaussian 09, Revision D.01, M. J. Frisch, G. W. Trucks, H. B. Schlegel, G. E. Scuseria, M. A. Robb, J. R. Cheeseman, G. Scalmani, V. Barone, G. A. Petersson, H. Nakatsuji, X. Li, M. Caricato, A. Marenich, J. Bloino, B. G. Janesko, R. Gomperts, B. Mennucci, H. P. Hratchian, J. V. Ortiz, A. F. Izmaylov, J. L. Sonnenberg, D. Williams-Young, F. Ding, F. Lipparini, F. Egidi, J. Goings, B. Peng, A. Petrone, T. Henderson, D. Ranasinghe, V. G. Zakrzewski, J. Gao, N. Rega, G. Zheng, W. Liang, M. Hada, M. Ehara, K. Toyota, R. Fukuda, J. Hasegawa, M. Ishida, T. Nakajima, Y. Honda, O. Kitao, H. Nakai, T. Vreven, K. Throssell, J. A. Montgomery, Jr., J. E. Peralta, F. Ogliaro, M. Bearpark, J. J. Heyd, E. Brothers, K. N. Kudin, V. N. Staroverov, T. Keith, R. Kobayashi, J. Normand, K. Raghavachari, A. Rendell, J. C. Burant, S. S. Iyengar, J. Tomasi, M. Cossi, J. M. Millam, M. Klene, C. Adamo, R. Cammi, J. W. Ochterski, R. L. Martin, K. Morokuma, O. Farkas, J. B. Foresman, and D. J. Fox, Gaussian, Inc., Wallingford CT, 2016.

[7] Becke, A.D. Density-functional thermochemistry. III. The role of exact exchange. *J. Chem. Phys.*, **1993**, *98*, 5648−5652

[8] Lee, C.; Yang, W.; Parr, R. G. Development of the Colle-Salvetti correlation-energy formula into a functional of the electron density. *Phys. Rev. B* **1988**, *37*, 785−789

[9] Zhao, Y.; Truhlar, D. The M06 suite of density functionals for main group thermochemistry, thermochemical kinetics, noncovalent interactions, excited states, and transition elements: two new functionals and systematic testing of four M06-class functionals and 12 other functionals. *Theor. Chem. Acc*. **2008**, *120*, 215−241.

[10] McLean, A. D.; Chandler, G. S. Contracted Gaussian basis sets for molecular calculations. I. Second row atoms, Z = 11−18. *J. Chem.Phys*. **1980**, *72*, 5639−5648.

[11] Krishnan, R.; Binkley, J. S.; Seeger, R.; Pople, J. A. Self-Consistent Molecular-Orbital Methods.20. Basis Set for Correlated Wave-Functions. *J. Chem. Phys.* **1980**, *72*, 650−654.

[12] Binning, R. C.; Curtiss, L. A. Compact contracted basis sets for third-row atoms: Ga−Kr. *J. Comput. Chem*. **1990**, *11*, 1206−1216.

[13] Hay, P. J.; Wadt, W. R. Ab initio effective core potentials for molecular calculations – potentials for the transition-metal atoms Sc to Hg. *J. Chem. Phys.*, **1985**, *82*, 270−283.

[14] Wadt, W. R.; Hay, P. J. Ab initio effective core potentials for molecular calculations – potentials for main group elements Na to Bi. *J. Chem. Phys.*, **1985**, *82*, 284−298.

[15] Hay, P. J.; Wadt, W. R. Ab initio effective core potentials for molecular calculations – potentials for K to Au including the outermost core orbitals. *J. Chem. Phys.*, **1985**, *82*, 299−310.

[16] Marenich, A. V.; Cramer, C. J.; Truhlar, D. G. Universal Solvation Model Based on Solute Electron Density and on a Continuum Model of the Solvent Defined by the Bulk Dielectric Constant and Atomic Surface Tensions. *J. Phys. Chem. B* **2009**, *113*, 6378−6396.

[17] Weigend, F.; Ahlrichs, R. Balanced basis sets of split valence, triple zeta valence and quadruple zeta valence quality for H to Rn: Design and assessment of accuracy. *Phys. Chem. Chem. Phys*. **2005**, *7*, 3297−3305.

[18] Weigend, F. Accurate Coulomb-fitting basis sets for H to Rn. *Phys. Chem. Chem. Phys.,* **2006**, *8*, 1057−1065

[19] Allouche, A-R. Gabedit—A graphical user interface for computational chemistry softwares. *J. Comput. Chem.* **2011**, *32*, 174–182

[20] Pyykkö, P.; Atsumi, M. Molecular Double-bond Covalent Radii for Elements Li-E112. *Chem. Eur. J*. **2009**, *15*, 12770−12779.